no results confirming the superiority of EGFR-TKI even showing clinical or genetic prediction of a better response, because these trials failed to show better survival over standard combination regimens including platinum agents.

We continue to await the results of research which will demonstrate clinical benefits in terms of survival even in selected patients, and which may help us to identify patients who are most likely to benefit from treatment with EGFR-TKI. Such results would tell us when and to whom we should prescribe the best drug to treat NSCLC.

REFERENCES

1 Parkin DM, Bray F, Ferlay J, Pisani P. Global cancer statistics, 2002. *CA Cancer J. Clin.* 2005; **55**: 74–108.
2 Schiller JH, Harrington D, Belani CP *et al.* Comparison of four chemotherapy regimens for advanced non-small-cell lung cancer. *N. Engl. J. Med.* 2002; **346**: 92–8.
3 Kelly K, Crowley J, Bunn PA Jr *et al.* Randomized phase III trial of paclitaxel plus carboplatin versus vinorelbine plus cisplatin in the treatment of patients with advanced non—small-cell lung cancer: a Southwest Oncology Group trial. *J. Clin. Oncol.* 2001; **19**: 3210–18.
4 Scagliotti GV, De Marinis F, Rinaldi M *et al.* Phase III randomized trial comparing three platinum-based doublets in advanced non-small-cell lung cancer. *J. Clin. Oncol.* 2002; **20**: 4285–91.
5 Kubota K, Nishiwaki Y, Ohashi Y *et al.* The Four-Arm Cooperative Study (FACS) for advanced non-small-cell lung cancer (NSCLC). *Proc. Am. Soc. Clin. Oncol.* 2004; **23**: Abstract 7006.
6 Fossella FV, Devore R, Kerr RN *et al.* Randomized phase III trial of docetaxel versus vinorelbine or ifosfamide in patients with advanced non-small-cell lung cancer previously treated with platinum-containing chemotherapy regimens. The TAX 320 Non-Small Cell Lung Cancer Study Group. *J. Clin. Oncol.* 2000; **18**: 2354–62.
7 Shepherd FA, Dancey J, Ramlau R *et al.* Prospective randomized trial of docetaxel versus best supportive care in patients with non-small-cell lung cancer previously treated with platinum-based chemotherapy. *J. Clin. Oncol.* 2000; **18**: 2095–103.
8 Hanna N, Shepherd FA, Fossella FV *et al.* Randomized phase III trial of pemetrexed versus docetaxel in patients with non-small-cell lung cancer previously treated with chemotherapy. *J. Clin. Oncol.* 2004; **22**: 1589–97.
9 Nakagawa K, Tamura T, Negoro S *et al.* Phase I pharmacokinetic trial of the selective oral epidermal growth factor receptor tyrosine kinase inhibitor gefitinib ('Iressa', ZD1839) in Japanese patients with solid malignant tumors. *Ann. Oncol.* 2003; **14**: 922–30.
10 Ranson M, Hammond LA, Ferry D *et al.* ZD1839, a selective oral epidermal growth factor receptor-tyrosine kinase inhibitor, is well tolerated and active in patients with solid, malignant tumors: results of a phase I trial. *J. Clin. Oncol.* 2002; **20**: 2240–50.
11 Herbst RS, Maddox AM, Rothenberg ML *et al.* Selective oral epidermal growth factor receptor tyrosine kinase inhibitor ZD1839 is generally well-tolerated and has activity in non-small-cell lung cancer and other solid tumors: results of a phase I trial. *J. Clin. Oncol.* 2002; **20**: 3815–25.
12 Baselga J, Rischin D, Ranson M *et al.* Phase I safety, pharmacokinetic, and pharmacodynamic trial of ZD1839, a selective oral epidermal growth factor receptor tyrosine kinase inhibitor, in patients with five selected solid tumor types. *J. Clin. Oncol.* 2002; **20**: 4292–302.
13 Fukuoka M, Yano S, Giaccone G *et al.* Multi-institutional randomized phase II trial of gefitinib for previously treated patients with advanced non-small-cell lung cancer (The IDEAL 1 Trial). *J. Clin. Oncol.* 2003; **21**: 2237–46.
14 Kris MG, Natale RB, Herbst RS *et al.* Efficacy of gefitinib, an inhibitor of the epidermal growth factor receptor tyrosine kinase, in symptomatic patients with non-small cell lung cancer: a randomized trial. *JAMA* 2003; **290**: 2149–58.
15 Perez-Soler R. Phase II clinical trial data with the epidermal growth factor receptor tyrosine kinase inhibitor erlotinib (OSI-774) in non-small-cell lung cancer. *Clin. Lung Cancer* 2004; **6** (Suppl. 1): S20–3.
16 Sirotnak FM, Zakowski MF, Miller VA, Scher HI, Kris MG. Efficacy of cytotoxic agents against human tumor xenografts is markedly enhanced by coadministration of ZD1839 (Iressa), an inhibitor of EGFR tyrosine kinase. *Clin. Cancer Res.* 2000; **6**: 4885–92.
17 Ciardiello F, Caputo R, Bianco R *et al.* Antitumor effect and potentiation of cytotoxic drugs activity in human cancer cells by ZD-1839 (Iressa), an epidermal growth factor receptor-selective tyrosine kinase inhibitor. *Clin. Cancer Res.* 2000; **6**: 2053–63.
18 Akita RW, Sliwkowski MX. Preclinical studies with Erlotinib (Tarceva). *Semin. Oncol.* 2003; **30** (3 Suppl. 7): 15–24.
19 Giaccone G, Herbst RS, Manegold C *et al.* Gefitinib in combination with gemcitabine and cisplatin in advanced non-small-cell lung cancer: a phase III trial—INTACT 1. *J. Clin. Oncol.* 2004; **22**: 777–84.
20 Herbst RS, Giaccone G, Schiller JH *et al.* Gefitinib in combination with paclitaxel and carboplatin in advanced non-small-cell lung cancer: a phase III trial—INTACT 2. *J. Clin. Oncol.* 2004; **22**: 785–94.
21 Gatzemeier U, Pluzanska A, Szczesna A *et al.* Results of a phase III trial of erlotinib (OSI-774) combined with cisplatin and gemcitabine (GC) chemotherapy in advanced non-small-cell lung cancer (NSCLC). *Proc. Am. Soc. Clin. Oncol.* 2004; **23**: Abstract 7010.
22 Herbst RS, Prager D, Hermann R *et al.* TRIBUTE: a phase III trial of erlotinib hydrochloride (OSI-774) combined with carboplatin and paclitaxel chemotherapy in advanced non-small-cell lung cancer. *J. Clin. Oncol.* 2005; **23**: 5892–9.
23 Thatcher N, Chang A, Parikh P *et al.* Gefitinib plus best supportive care in previously treated patients with refractory advanced non-small-cell lung cancer: results from a randomised, placebo-controlled, multicentre study (Iressa Survival Evaluation in Lung Cancer). *Lancet* 2005; **366**: 1527–37.
24 Shepherd FA, Rodrigues Pereira J, Ciuleanu T *et al.* Erlotinib in previously treated non-small-cell lung cancer. *N. Engl. J. Med.* 2005; **353**: 123–32.
25 Inoue A, Saijo Y, Maemondo M *et al.* Severe acute interstitial pneumonia and gefitinib. *Lancet* 2003; **361**: 137–9.

© 2006 The Authors
Journal compilation © 2006 Asian Pacific Society of Respirology

26 Ieki R, Saitoh E, Shibuya M. Acute lung injury as a possible adverse drug reaction related to gefitinib. *Eur. Respir. J.* 2003; **22**: 179–81.
27 Okamoto I, Fujii K, Matsumoto M *et al.* Diffuse alveolar damage after ZD1839 therapy in a patient with non-small cell lung cancer. *Lung Cancer* 2003; **40**: 339–42.
28 Han SW, Hwang PG, Chung DH *et al.* Epidermal growth factor receptor (EGFR) downstream molecules as response predictive markers for gefitinib (Iressa, ZD1839) in chemotherapy-resistant non-small cell lung cancer. *Int. J. Cancer* 2005; **113**: 109–15.
29 Chiu CH, Tsai CM, Chen YM, Chiang SC, Liou JL, Perng RP. Gefitinib is active in patients with brain metastases from non-small cell lung cancer and response is related to skin toxicity. *Lung Cancer* 2005; **47**: 129–38.
30 Ando M, Okamoto I, Yamamoto N *et al.* Predictive factors for interstitial lung disease, antitumor response, and survival in non-small-cell lung cancer patients treated with gefitinib. *J. Clin. Oncol.* 2006; **24**: 2549–56.
31 AstraZenecaKK. Final report on interstital lung disease (ILD) related to gefitinib (Iressa Tablet 250) by Iressa Expert Committee. AstraZenecaKK, Osaka, Japan, 2003.
32 Takano T, Ohe Y, Kusumoto M *et al.* Risk factors for interstitial lung disease and predictive factors for tumor response in patients with advanced non-small cell lung cancer treated with gefitinib. *Lung Cancer* 2004; **45**: 93–104.
33 Hotta K, Kiura K, Tabata M *et al.* Interstitial lung disease in Japanese patients with non-small cell lung cancer receiving gefitinib: an analysis of risk factors and treatment outcomes in Okayama Lung Cancer Study Group. *Cancer J.* 2005; **11**: 417–24.
34 Niho S, Kubota K, Goto K *et al.* First-line single agent treatment with gefitinib in patients with advanced non-small-cell lung cancer: a phase II study. *J. Clin. Oncol.* 2006; **24**: 64–9.
35 Cohen MH, Williams GA, Sridhara R *et al.* United States Food and Drug Administration Drug Approval summary: Gefitinib (ZD1839; Iressa) tablets. *Clin. Cancer Res.* 2004; **10**: 1212–18.
36 Camus P, Kudoh S, Ebina M. Interstitial lung disease associated with drug therapy. *Br. J. Cancer* 2004; **91** (Suppl. 2): S18–23.
37 Yoshida S. The results of gefitinib prospective investigation. *Med. Drug J.* 2005; **41**: 772–89.
38 Endo M, Johkoh T, Kimura K, Yamamoto N. Imaging of gefitinib-related interstitial lung disease: multi-institutional analysis by the West Japan Thoracic Oncology Group. *Lung Cancer* 2006; **52**: 135–40.
39 Miller VA, Kris MG, Shah N *et al.* Bronchioloalveolar pathologic subtype and smoking history predict sensitivity to gefitinib in advanced non-small-cell lung cancer. *J. Clin. Oncol.* 2004; **22**: 1103–9.
40 Lynch TJ, Bell DW, Sordella R *et al.* Activating mutations in the epidermal growth factor receptor underlying responsiveness of non-small-cell lung cancer to gefitinib. *N. Engl. J. Med.* 2004; **350**: 2129–39.
41 Paez JG, Janne PA, Lee JC *et al.* EGFR mutations in lung cancer: correlation with clinical response to gefitinib therapy. *Science* 2004; **304**: 1497–500.
42 Takano T, Ohe Y, Sakamoto H *et al.* Epidermal growth factor receptor gene mutations and increased copy numbers predict gefitinib sensitivity in patients with recurrent non-small-cell lung cancer. *J. Clin. Oncol.* 2005; **23**: 6829–37.
43 Mitsudomi T, Kosaka T, Endoh H *et al.* Mutations of the epidermal growth factor receptor gene predict prolonged survival after gefitinib treatment in patients with non-small-cell lung cancer with postoperative recurrence. *J. Clin. Oncol.* 2005; **23**: 2513–20.
44 Han SW, Kim TY, Hwang PG *et al.* Predictive and prognostic impact of epidermal growth factor receptor mutation in non-small-cell lung cancer patients treated with gefitinib. *J. Clin. Oncol.* 2005; **23**: 2493–501.
45 Pao W, Miller V, Zakowski M *et al.* EGF receptor gene mutations are common in lung cancers from 'never smokers' and are associated with sensitivity of tumors to gefitinib and erlotinib. *Proc. Natl. Acad. Sci. USA* 2004; **101**: 13306–11.
46 Huang SF, Liu HP, Li LH *et al.* High frequency of epidermal growth factor receptor mutations with complex patterns in non-small cell lung cancers related to gefitinib responsiveness in Taiwan. *Clin. Cancer Res.* 2004; **10**: 8195–203.
47 Cappuzzo F, Hirsch FR, Rossi E *et al.* Epidermal growth factor receptor gene and protein and gefitinib sensitivity in non-small-cell lung cancer. *J. Natl. Cancer Inst.* 2005; **97**: 643–55.
48 Hirsch FR, Varella-Garcia M, Mccoy J *et al.* Increased epidermal growth factor receptor gene copy number detected by fluorescence in situ hybridization associates with increased sensitivity to gefitinib in patients with bronchioloalveolar carcinoma subtypes: a Southwest Oncology Group Study. *J. Clin. Oncol.* 2005; **23**: 6838–45.
49 Tsao MS, Sakurada A, Cutz JC *et al.* Erlotinib in lung cancer—molecular and clinical predictors of outcome. *N. Engl. J. Med.* 2005; **353**: 133–44.
50 Cappuzzo F, Magrini E, Ceresoli GL *et al.* Akt phosphorylation and gefitinib efficacy in patients with advanced non-small-cell lung cancer. *J. Natl. Cancer Inst.* 2004; **96**: 1133–41.
51 Pao W, Wang TY, Riely GJ *et al.* KRAS mutations and primary resistance of lung adenocarcinomas to gefitinib or erlotinib. *PLoS Med.* 2005; **2**: e17.
52 Eberhard DA, Johnson BE, Amler LC *et al.* Mutations in the epidermal growth factor receptor and in KRAS are predictive and prognostic indicators in patients with non-small-cell lung cancer treated with chemotherapy alone and in combination with erlotinib. *J. Clin. Oncol.* 2005; **23**: 5900–9.
53 Kobayashi S, Boggon TJ, Dayaram T *et al.* EGFR mutation and resistance of non-small-cell lung cancer to gefitinib. *N. Engl. J. Med.* 2005; **352**: 786–92.
54 Pao W, Miller VA, Politi KA *et al.* Acquired resistance of lung adenocarcinomas to gefitinib or erlotinib is associated with a second mutation in the EGFR kinase domain. *PLoS Med.* 2005; **2**: e73.

© 2006 The Authors
Journal compilation © 2006 Asian Pacific Society of Respirology

Oncogene (2006), 1–11
© 2006 Nature Publishing Group All rights reserved 0950-9232/06 $30.00
www.nature.com/onc

ORIGINAL ARTICLE

Akt-dependent nuclear localization of Y-box-binding protein 1 in acquisition of malignant characteristics by human ovarian cancer cells

Y Basaki[1,2], F Hosoi[1,3,4], Y Oda[2], A Fotovati[4], Y Maruyama[4], S Oie[1,2], M Ono[1,3,4], H Izumi[5], K Kohno[5], K Sakai[6], T Shimoyama[6], K Nishio[6] and M Kuwano[1,4]

[1]Station-II for Collaborative Research, Kyushu University, Fukuoka, Japan; [2]Department of Anatomic Pathology, Graduate School of Medical Sciences, Kyushu University, Fukuoka, Japan; [3]Medical Biochemistry, Graduate School of Medical Sciences, Kyushu University, Fukuoka, Japan; [4]Research Center for Innovative Cancer Therapy, Kurume University, Kurume, Japan; [5]Department of Molecular Biology, University of Occupation and Environmental Health, Kitakyushu, Japan and [6]Pharmacology Division, National Cancer Center Research Institute, Tokyo, Japan

Y-box-binding protein 1 (YB-1), which is a member of the DNA-binding protein family containing a cold-shock domain, has pleiotropic functions in response to various environmental stimuli. As we previously showed that YB-1 is a global marker of multidrug resistance in ovarian cancer and other tumor types. To identify YB-1-regulated genes in ovarian cancers, we investigated the expression profile of YB-1 small-interfering RNA (siRNA)-transfected ovarian cancer cells using a high-density oligonucleotide array. YB-1 knockdown by siRNA upregulated 344 genes, including *MDR1*, *thymidylate synthetase*, *S100 calcium binding protein* and *cyclin B*, and downregulated 534 genes, including *CXCR4*, *N-myc downstream regulated gene 1*, *E-cadherin* and *phospholipase C*. Exogenous serum addition stimulated YB-1 translocation from the cytoplasm to the nucleus, and treatment with Akt inhibitors as well as Akt siRNA and integrin-linked kinase (ILK) siRNA specifically blocked YB-1 nuclear localization. Inhibition of Akt activation downregulated *CXCR4* and upregulated *MDR1* (*ABCB1*) gene expression. Administration of Akt inhibitor resulted in decrease in nuclear YB-1-positive cancer cells in a xenograft animal model. Akt activation thus regulates the nuclear translocation of YB-1, affecting the expression of drug-resistance genes and other genes associated with the malignant characteristics in ovarian cancer cells. Therefore, the Akt pathway could be a novel target of disrupting the nuclear translocation of YB-1 that has important implications for further development of therapeutic strategy against ovarian cancers.
Oncogene advance online publication, 30 October 2006; doi:10.1038/sj.onc.1210084

Keywords: Akt; microarray; ovarian carcinoma; Y-box-binding protein-1

Correspondence: Dr Y Basaki, Station-II for Collaborative Research, Kyushu Univeristy, 3-1-1 Maidashi, Higashi-ku, Fukuoka 812-8582, Japan.
E-mail: yubasaki@yahoo.co.jp
Received 28 February 2006; revised 25 August 2006; accepted 11 September 2006

Introduction

The Y-box-binding protein 1 (YB-1), which is a DNA/RNA-binding protein also known as dbpB, regulates transcription, translation, DNA damage repair and other biological processes in both the nucleus and cytoplasm (Matsumoto and Wolffe, 1998; Kohno *et al.*, 2003). In the cytoplasm, YB-1 regulates mRNA stability and translational regulation (Evdokimova *et al.*, 2001; Ashizuka *et al.*, 2002; Fukuda *et al.*, 2004), while in the nucleus, it plays a pivotal role in transcriptional regulation through specific recognition of the Y-box promoter element (Ladomery and Sommerville, 1995; Kohno *et al.*, 2003). Interaction of YB-1 with its cognate Y-box-binding site (inverted CCAAT box) is promoted by cytotoxic stimuli, including actinomycin D, cisplatin, etoposide, ultraviolet (UV) and heat shock, leading to the activation of a representative ABC transporter *MDR1/ABCB1* and DNA topoisomerase IIα genes (Asakuno *et al.*, 1994; Furukawa *et al.*, 1998; Ohga *et al.*, 1998). YB-1 also selectively interacts with damaged DNA or RNA, and protects from cytotoxic effects following cellular exposure to cisplatin, mitomycin C, UV and oxygen radicals (Ohga *et al.*, 1996; Ise *et al.*, 1999).

Royer and co-workers were the first to report that nuclear localization of YB-1 is associated with intrinsic *MDR1* expression in human primary breast cancer (Bargou *et al.*, 1997). Immunostaining analysis of various human cancers also supported this result, and showed that nuclear expression of activated YB-1 was closely associated with the acquisition of P-glycoprotein-mediated multidrug resistance (Kuwano *et al.*, 2004). YB-1 has also been shown to induce basal and 5-fluorouracil-induced expression of the major vault protein (*MVP/LRP*) gene, the promoter of which contains a Y-box (Stein *et al.*, 2005). In human malignancies, vault proteins are involved in acquiring drug resistance (Mossink *et al.*, 2003). Taken together, these findings suggest that nuclear localization of YB-1 might play a key role in the acquisition of global drug resistance through transcriptional activation of relevant genes and the repair of damaged DNA (Kuwano *et al.*, 2004).

The nuclear localization of YB-1 is required for transcription and DNA repair in response to various environmental stimuli, such as adenovirus infection (Holm *et al.*, 2002), DNA-damaging agents, UV irradiation, hyperthermia (Stein *et al.*, 2001) and serum stimulation (En-Nia *et al.*, 2005). However, as a nucleocytoplasmic shuttling protein, it is important to understand which signalling molecules are involved in the translocation of YB-1 into the nucleus. Koike *et al.* (1997) first reported the possible role of protein kinase C in YB-1 nuclear translocation in cancer cells exposed to UV irradiation, and highlighted the importance of the YB-1 C-terminal region in cytoplasmic retention. Other studies have suggested the involvement of additional molecules: thrombin-mediated YB-1 nuclear translocation was shown to be inhibited by protein tyrosine phosphatase inhibitor in endothelial cells (Stenina *et al.*, 2000), while Dooley *et al.* (2006) demonstrated the involvement of Jak1 in YB-1 nuclear translocation. Sutherland *et al.* (2005) recently reported that phosphorylation of YB-1 by Akt at serine 102 in the cold-shock domain is required for YB-1 nuclear translocation in cancer cells. Another mechanism for nuclear translocation of YB-1 was shown to be promoted by various cytotoxic anticancer agents, which trigger the proteolytic cleavage by the 20S proteasome of the YB-1 C-terminal fragment containing the cytoplasmic retention signal (Sorokin *et al.*, 2005). In our present study, we have provided evidence that Akt activation is one of the mechanisms for nuclear translocalization of YB-1, and also that YB-1 regulates expression of various cell growth and malignant progression-related genes as well as global drug resistance-related genes including *MDR1*.

Results

Suppression of YB-1 leads to an enhancement of MDR-1 expression and decrease of CXCR-4 expression

We previously reported that YB-1 was expressed in the nucleus in almost 30% of serous ovarian cancers, and that YB-1 nuclear-positive patients had a poor prognosis (Kamura *et al.*, 1999). As nuclear translocation of YB-1 is highly susceptible to environmental stimuli, we first examined whether the stress-inducing exogenous addition of serum could stimulate nuclear translocation of YB-1 in seven serum-deprived human ovarian cancer cell lines. Among the seven cell lines, nuclear YB-1 translocation was stimulated more than twofold in two: RMG-III and SKOV-3 (Figure 1a). In these two lines, serum incubation markedly enhanced Akt phosphorylation and increased translocation of YB-1 into the

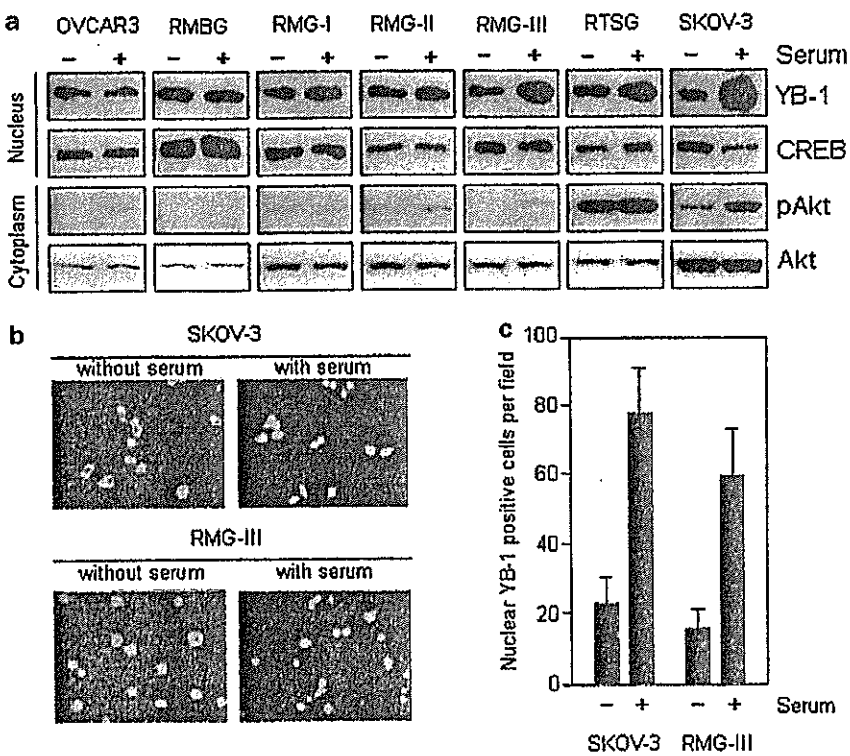

Figure 1 Levels of Akt phosphorylation and nuclear localization of YB-1 in ovarian cancer cell lines with or without serum stimulation. (a) Cytoplasmic and nuclear extracts were prepared 1 h after 10% serum stimulation. Anti-YB-1 and anti-CREB immunoblots were performed on nuclear extracts, and anti-pAkt and anti-Akt immunoblots were performed with cytoplasmic extracts. CREB and Akt are shown as a loading control. (b) Immunofluorescent staining of YB-1 in ovarian cancer cells. Cells stimulated with or without serum for 1 h were fixed and permeabilized, incubated at 4°C with the primary YB-1 antibody, then with the Alexa Flour 546-labelled secondary antibody. (c) Quantitative analysis of YB-1 nuclear localization as shown in Figure 1b. Data are mean of three independent experiments; bars ±s.d.

nucleus, as shown by immunofluorescense analysis (Figure 1b and c).

Although YB-1 is known to regulate the expression of several genes at the transcriptional level, the complete network of genes associated with YB-1 has not been elucidated. We therefore, explored the expression profile of YB-1 siRNA-treated SKOV-3 cells and mock-treated SKOV-3 cells using a high-density oligonucleotide microarray. We transfectd YB-1 siRNA into SKOV-3 cells at a concentration of 200 and 400 nM. Transfection of 200 nM YB-1 siRNA decreased expression of YB-1 mRNA by only 45%, whereas 400 nM YB-1 siRNA decreased by 70% (Figure 2). Of the 54675 RNA transcripts and variants in the microarray, we identified 344 genes that were increased more than twofold and 534 genes that were decreased 0.5-fold or less in both 200 and 400 nM YB-1 siRNA-transfected cells (Supplementary Table S1). Upregulated genes were classified into 'cell cycle' ($P<0.0001$), 'cytoskeleton organization and biogenesis' ($P=0.0003$), 'cell growth and/or maintenance' ($P=0.0005$), and GO SLIMS Biological Process' ($P=0.0013$). Downregulated genes were classified into 'catalytic activity' ($P=0.0007$) and 'transferase' ($P=0.0010$). We selected 46 genes that we expected to be associated with drug resistance, cell growth, cancer malignant progression and cell signalling (Table 1), and chose three of these for further study: *MDR1*, *MVP/LRP* and chemokine (C-X-C motif) receptor 4 (*CXCR4*).

We used quantitative real-time PCR (QRT-PCR) to confirm whether expression of these three genes was modulated in YB-1 siRNA-transfected cells. Expression of *CXCR4* decreased by 67%, whereas expression of *MVP/LRP* was unaffected by the siRNA (Figure 2). *MDR1* expression was increased approximately 30-fold in 400 nM YB-1 siRNA-transfected cells compared with control siRNA-transfected cells. The results of QRT-PCR are broadly consistent with those of the microarray analysis.

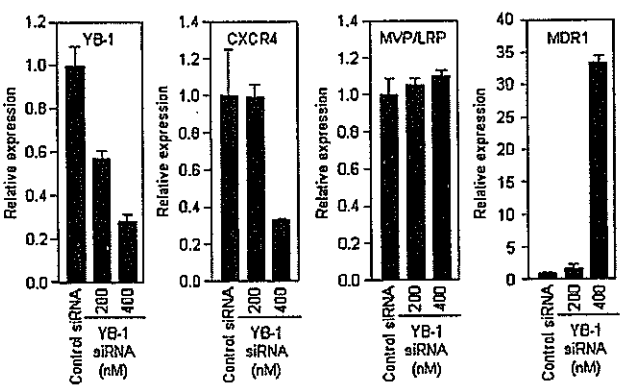

Figure 2 Effect of YB-1 knock down on expression of MDR1, MVP/LRP and CXCR4. SKOV-3 cells were treated with YB-1 siRNA for 48 h and then total RNA was prepared. QRT-PCR was performed for MDR1, MVP/LRP, CXCR4, YB-1 and housekeeping gene glyceraldehyde-3-phosphate dehydrogenase (GAPDH). The relative gene expression for each sample was determined using the formula $2^{(-\Delta C_t)} = 2^{(C_t(\text{GAPDH})-C_t(\text{target}))}$ which reflected target gene expression normalized to GAPDH levels. Data were mean of three independent experiments; bars ± s.d.

Pearson correlation and hierarchical cluster analysis of selected NCI-60 genes

We next examined a database containing the expression profile of the National Cancer Institute (NCI)-60 panel from the Developmental Therapeutics Program (http://www.dtp. nci.nih.gov/), shown as a log of mRNA expression level in the NCI screen. When the Pearson correlation coefficients were calculated, YB-1 was negatively correlated with *MDR1* expression, positively correlated with *CXCR4* expression and showed little correlation with *MVP/LRP* (Figure 3). Moreover, the hierarchical dendrogram of gene expression revealed that *YB-1* and *CXCR4* belong to the same cluster, whereas *MDR1* and *MVP/LRP* are clustered in a separate group (Figure 4). Together, these NCI-60 panels suggest that cellular levels of YB-1 negatively modulate expression of *MDR1* and positively regulate expression of *CXCR4*. In this cluster analysis, six ovarian cancer cell lines including SKOV-3 showed various correlation coefficiencies with YB-1 expression. Our oligonucleotide array analysis was performed only with SKOV-3, and correlation coefficiencies among ovarian cancer cell lines would depend upon which cell line was analysed.

Akt activity is prerequisite for nuclear translocation of YB-1and transcriptional regulation by YB-1

Phosphorylation of YB-1 by Akt is a necessary requirement for its translocation from the cytoplasm into the nucleus (Sutherland *et al.*, 2005). We therefore investigated the effect of two inhibitors of Akt activation (LY294002 and 1L-6-hydroxymethyl-*chiro*-inositol 2(*R*)-2-*O*-methyl-3-*O*-octadecylcarbonate) on serum-stimulated SKOV-3 cells. Both Akt inhibitors markedly blocked the nuclear accumulation of YB-1, whereas treatment with inhibitors of MEK (U0126), p38MAPK (SB203580) and JNK (SP600125) had no effect on nuclear translocation (Figure 5a). In addition, phosphorylation of Akt was inhibited by LY294002 and octadecylcarbonate, but not by U0126, SB203580 and SP600125. Immunofluorescence analysis with a YB-1 antibody also demonstrated the predominant accumulation of YB-1 in the cytoplasm when treated with LY294002 and octadecylcarbonate (Figure 5b and c). As Akt inhibitors blocked the nuclear translocation of YB-1, we examined whether they could also affect expression of YB-1-regulated genes. *CXCR4* expression was found to be downregulated in a dose-dependent manner following treatment with the Akt inhibitors when determined by QRT-PCR analysis (Figure 5d). Treatment with Akt inhibitors upregulated the expression of *MDR1*, but not *MVP/LRP*.

SKOV-3 cells expressed high level of Akt1 protein, very low level of Akt2 protein, and no Akt3 protein when assayed by immunoblotting analysis (Figure 6a). We introduced siRNA targeting Akt or ILK into SKOV-3 cells at a concentration of 100 and 10 nM,

Table 1 List of genes differentially expressed in YB-1 siRNA-transfected SKOV-3 cells

Unigene	*Accession*	*Symbol*	*Description*	*Mean fold change*
Hs.489033	NM_000927	ABCB1	MDR1, ATP-binding cassette, sub-family B (MDR/TAP), member 1	2.46
Hs.369762	AB077208	TYMS	Thymidylate synthetase	1.71
Hs.198363	NM_018518	MCM10	MCM10 minichromosome maintenance deficient 10	1.70
Hs.405958	U77949	CDC6	CDC6 cell division cycle 6 homolog (*S. cerevisiae*)	1.66
Hs.442658	AB011446	AURKB	Aurora kinase B	1.65
Hs.516484	NM_005978	S100A2	S100 calcium-binding protein A2	1.48
Hs.23960	NM_031966	CCNB1	Cyclin B1	1.40
Hs.460184	AA604621	MCM4	MCM4 minichromosome maintenance deficient 4 (*S. cerevisiae*)	1.40
Hs.438720	AF279900	MCM7	MCM7 minichromosome maintenance deficient 7 (*S. cerevisiae*)	1.36
Hs.433168	NM_002960	S100A3	S100 calcium binding protein A3	1.33
Hs.115474	NM_002915	RFC3	Replication factor C (activator 1) 3, 38 kDa	1.28
Hs.122908	NM_030928	CDT1	DNA replication factor	1.28
Hs.329989	NM_005030	PLK1	Polo-like kinase 1 (*Drosophila*)	1.21
Hs.334562	NM_001786	CDC2	Cell division cycle 2, G1 to S and G2 to M	1.21
Hs.74034	NM_001753	CAV1	Caveolin 1, caveolae protein, 22 kDa	1.19
Hs.477481	NM_004526	MCM2	MCM2 minichromosome maintenance deficient 2, mitotin	1.16
Hs.284244	M27968	FGF2	Fibroblast growth factor 2 (basic)	1.10
Hs.179565	NM_002388	MCM3	MCM3 minichromosome maintenance deficient 3 (*S. cerevisiae*)	1.08
Hs.194698	NM_004701	CCNB2	Cyclin B2	1.04
Hs.506989	BC001866	RFC5	Replication factor C (activator 1) 5, 36.5 kDa	1.02
Hs.171596	NM_004431	EPHA2	EPH receptor A2	1.01
Hs.194143	NM_007294	BRCA1	Breast cancer 1, early onset	0.75
Hs.156346	NM_001067	TOP2A	Topoisomerase (DNA) II alpha 170 kDa	0.64
Hs.473163	NM_001719	BMP7	Bone morphogenetic protein 7 (osteogenic protein 1)	0.54
Hs.391464	NM_004996	ABCC1	MRP-1, ATP-binding cassette, sub-family C (CFTR/MRP), member 1	0.20
Hs.256301	NM_199249	MGC13170	Multidrug resistance-related protein	0.15
Hs.513488	NM_017458	MVP	Major vault protein	−0.05
Hs.482526	NM_014886	TINP1	TGF beta-inducible nuclear protein 1	−0.23
Hs.525557	NM_000295	SERPINA1	Serpin peptidase inhibitor, clade A (alpha-1 antiproteinase, antitrypsin), member	−1.01
Hs.500466	BG403361	PTEN	Phosphatase and tensin homolog (mutated in multiple advanced cancers 1)	−1.05
Hs.25292	NM_002229	JUNB	Jun B proto-oncogene	−1.06
Hs.132225	AI934473	PIK3R1	Phosphoinositide-3-kinase, regulatory subunit, polypeptide 1 (p85 alpha)	−1.16
Hs.83169	NM_002421	MMP1	Matrix metalloproteinase 1 (interstitial collagenase)	−1.22
Hs.508999	NM_002742	PRKCM	Protein kinase C, mu	−1.29
Hs.326035	NM_001964	EGR1	Early growth response 1	−1.29
Hs.2256	NM_002423	MMP7	Matrix metalloproteinase 7 (matrilysin, uterine)	−1.32
Hs.197922	NM_018584	CaMKIINalpha	Calcium/calmodulin-dependent protein kinase II	−1.36
Hs.132966	AA005141	MET	Met proto-oncogene (hepatocyte growth factor receptor)	−1.39
Hs.208124	NM_000125	ESR1	Estrogen receptor 1	−1.50
Hs.73793	M27281	VEGF	Vascular endothelial growth factor	−1.53
Hs.381167	AW512196	SERPINB1	Serine (or cysteine) proteinase inhibitor, clade B (ovalbumin), member 1	−1.70
Hs.413111	NM_002661	PLCG2	Phospholipase C, gamma 2 (phosphatidylinositol-specific)	−1.75
Hs.461086	NM_004360	CDH1	Cadherin 1, type 1, E-cadherin (epithelial)	−1.92
Hs.472793	AI631895	SGK2	Serum/glucocorticoid regulated kinase 2	−2.04
Hs.372914	NM_006096	NDRG1	*N-myc* downstream regulated gene 1	−2.34
Hs.421986	NM_001008540	CXCR4	Chemokine (C-X-C motif) receptor 4	−2.64

High-density oligonucleotide array was performed on 400 nM YB-1 siRNA-treated SKOV-3 cells and mock-treated cells. siRNA duplexes were transfected using LipofectAMINE2000 with Opti-MEM mediums. At 48 h after siRNA transfection, total RNA was prepared, and subjected to double-stranded cDNA synthesis and *in vitro* transcription. The labeled cRNA was applied to the oligonucleotide microarray.

respectively, and silencing effects of siRNA were analysed by immunoblotting (Figure 6a). In Akt siRNA almost completely silenced both Akt1 and Akt2, and siRNA for ILK, the upstream kinase for Akt, silenced ILK on protein level. Treatment with Akt siRNA and ILK siRNA resulted in a marked decrease in both pAkt expression and nuclear accumulation of YB-1 (Figure 6a). As both Akt and ILK siRNA blocked the nuclear translocation of YB-1, we examined their effects on expression of YB-1-regulated genes (Figure 6b). Treatment with Akt and ILK siRNA downregulated the expression of *CXCR4* gene, and upregulated the expression of *MDR1* gene. By contrast there appeared no marked effect on the expression of *MVP/LRP* and *YB-1* genes when treated with both siRNAs (Figure 6b).

Effect of LY294002 treatment on Akt phosphorylation and YB-1 nuclear localization in SKOV-3 xenograft

To further investigate the involvement of Akt in tumoural YB-1 nuclear localization, an *in vivo* xenograft

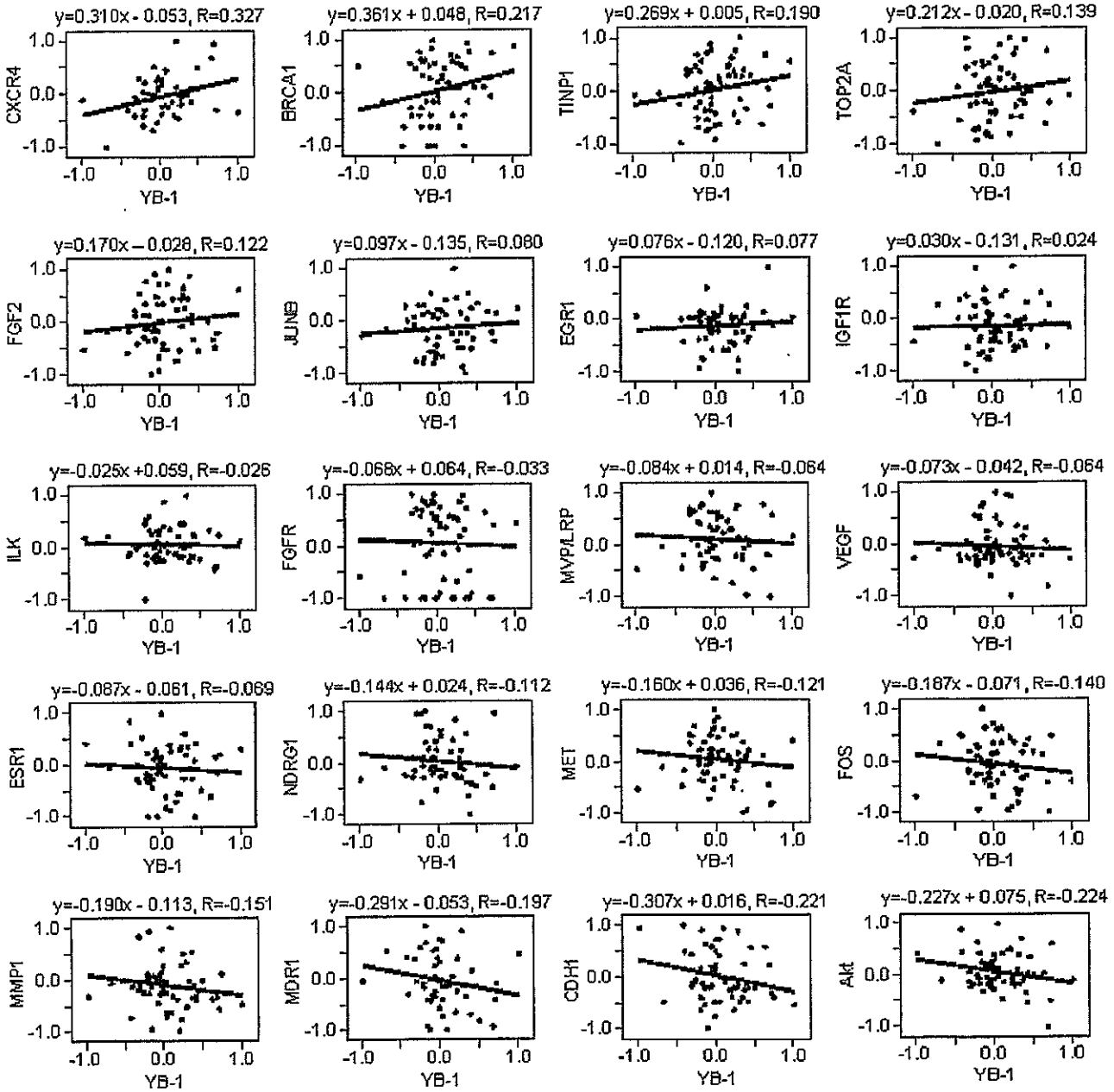

Figure 3 Correlation analysis of gene expression in NCI-60 screen. Gene expression data for the 60 human tumor cell lines were obtained from the Developmental Therapeutics Program (http://www.dtp.nci.nih.gov/), expressed as log of the mRNA levels in cell line/mRNA levels in reference pool in the NCI screen. Pearson correlation coefficients were calculated for each gene–gene pair.

assay was performed. Administration of LY294002 (i.p.) to mice carrying SKOV-3 cell tumors inhibited the phosphorylation of Akt (Figure 7a and b). Akt phosphorylation and YB-1 nuclear localization were also evaluated by immunohistochemical analysis. Tumors in the LY294002-treated group displayed a lower level of pAkt staining (3.3 ± 0.5) than those in the control group, where the mean number of nuclear YB-1-positive cells was 24.7 ± 3.4 (Figure 7c and d). Taken together, these results suggest that nuclear localization of YB-1 in ovarian cancer cells is closely associated with Akt phosphorylation activity *in vitro* and *in vivo*.

Discussion

The nuclear localization of YB-1 is essential process for YB-1-driven transcription of various genes and DNA repair in cancer cells in response to various environmental stimuli. One should understand which signalling pathway specifically controls the translocation of YB-1 from cytoplasm into nucleus. Our previous study has demonstrated that PKC activates the nuclear localization of YB-1 in cancer cells treated with UV irradiation or cisplatin, and also that the C-terminal region of YB-1 was important for its cytoplasmic

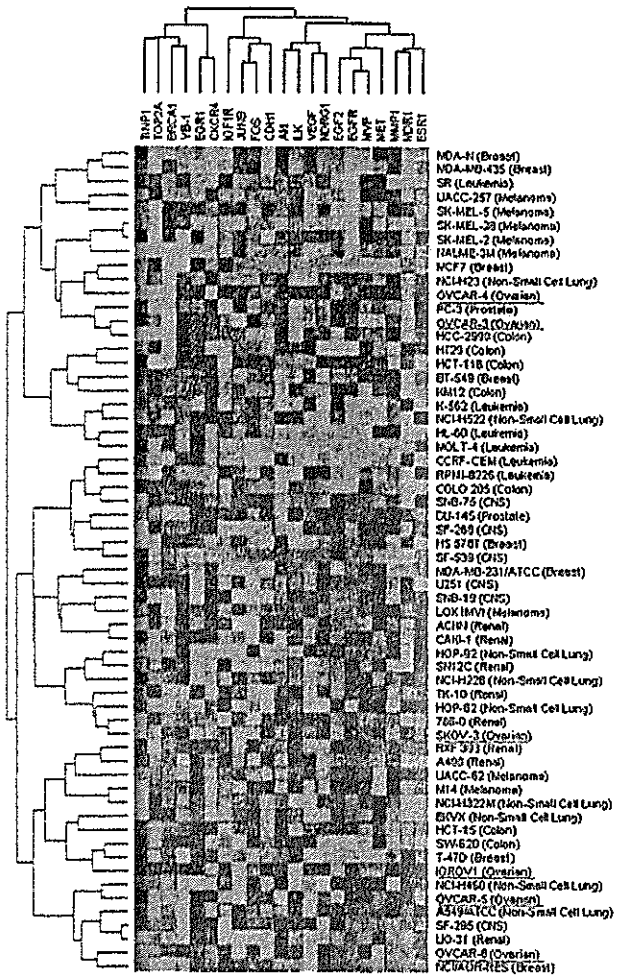

Figure 4 Hierarchical clustering of gene expression in NCI-60 screen. Hierarchical clustering can be used to group cell lines and genes in term of their patterns of gene expression. To obtain cluster trees for genes that showed distinct expression patterns across the 60 cell lines, we used the program 'Cluster' and 'Tree View' (http://rana.lbl.gov/) with average linkage clustering and a correlation metric.

retention (Koike *et al.*, 1997). Sutherland *et al.* (2005) have presented more definitive mechanism at molecular basis that phosphorylation of serine 102 at cold-shock domain of YB-1 by Akt is essential for the nuclear YB-1 localization in breast cancer cells, and also that ILK phosphorylate its downstream Akt, resulting in activation of YB-1 and it nuclear localization. Consistent with this study, our present study also demonstrated that Akt as well as ILK played a critical role in the nuclear YB-1 localization and YB-1-driven-transcriptional control of various genes including *CXCR4* and *MDR1* in human ovarian cancer cells.

In our present study, we examined whether expression of two multidrug resistance relevant genes, *MVP/LRP* and *MDR1/ABCB1*, was affected by knockdown of YB-1. Stein *et al.* (2005) have reported that the *MVP/LRP* gene is transcriptionally activated by YB-1 in response to cytotoxic anticancer agents including doxorubicin and 5-fluorouracil: *MVP/LRP* is an essential vault protein involving acquirement of multidrug resistance. However, in ovarian cancer cells, there was no causative association between the two genes when assayed by microarray and QRT-PCR. YB-1 might not regulate *MVP/LRP* expression in ovarian cancer cells used in our present study. In contrast, in human breast cancer cells, treatment with YB-1 siRNA markedly upregulated *MVP/LRP* expression (Shimoyama T, Nishio K, Basaki Y, Ono M and Kuwano M, unpublished data), suggesting that YB-1-induced regulation of *MVP/LRP* gene expression depends upon cancer cell types and/or types of stimuli. In contrast, knockdown or nuclear translocation inhibition of YB-1 upregulated expression of another drug resistance *MDR1* gene in ovarian cancer cells. Various environmental stimuli often upregulated *MDR1* gene in various human cancer cells through pleiotropic transcriptional regulations (Kuwano *et al.*, 2004). Our present study further presented a novel regulation of YB-1-induced negative control of *MDR1* gene in ovarian cancer cells, and further study should be required to understand its underlying mechanism at molecular basis.

In our present study, we first observed that the knockdown of YB-1, ILK and Akt as well as an Akt inhibitor all downregulated expression of *CXCR4* gene. Consistent with recent study by Sutherland *et al.* (2005), ILK-Akt activation could be responsible for the nuclear localization of YB-1, resulting in enhanced expression of *CXCR4* gene. The 2.6 Kb 5′-flanking region located upstream of the *CXCR4* gene contains a TATA box and the transcription start site characteristic of a functional promoter (Caruz *et al.*, 1998) and this region also contained putative consensus Y-box-binding site (inverted CCAAT box) form −685 to −681. However, it remains unknown whether ILK-Akt-induced activation of YB-1 is directly involved in the upregulation of *CXCR4* gene.

CXCL12 (SDF-1α) is a specific ligand of CXCR4. CXCL12 induced a dose dependent proliferation of human ovarian cancer cells through its specific interaction with CXCR4 (Porcile *et al.*, 2005). This CXCR4 activation by CXCL12 further stimulated EGF receptor phosphorylation and its downstream kinases, ERK1/2, Akt and c-Src that might link several signallings of cell proliferation in ovarian cancer cells (Porcile *et al.*, 2005). On the other hand, VEGF, a potent angiogenic factor, induced upregulation of *CXCR4* gene expression in vascular endothelial cells, and expression of both VEGF and CXCL12 was very high in ascites of patients with advanced ovarian cancers (Kryczek *et al.*, 2005). The cross-talk of CXCL12/CXCR4 with EGF/EGF receptor and/or VEGF/VEGF receptor might thus provide important signallings for both cell proliferation and angiogenesis in ovarian cancers.

CXCL12/CXCR4 pathway is also expected to be clinically involved in acquirement of malignant characteristics of human ovarian cancers. Of 14 chemokine receptors, only CXCR4 protein was found to be expressed in ovarian cancer cell lines and in ascites from patients with ovarian cancers (Scotton *et al.*, 2001). The CXCL12/CXCR4 pathway has been implicated in

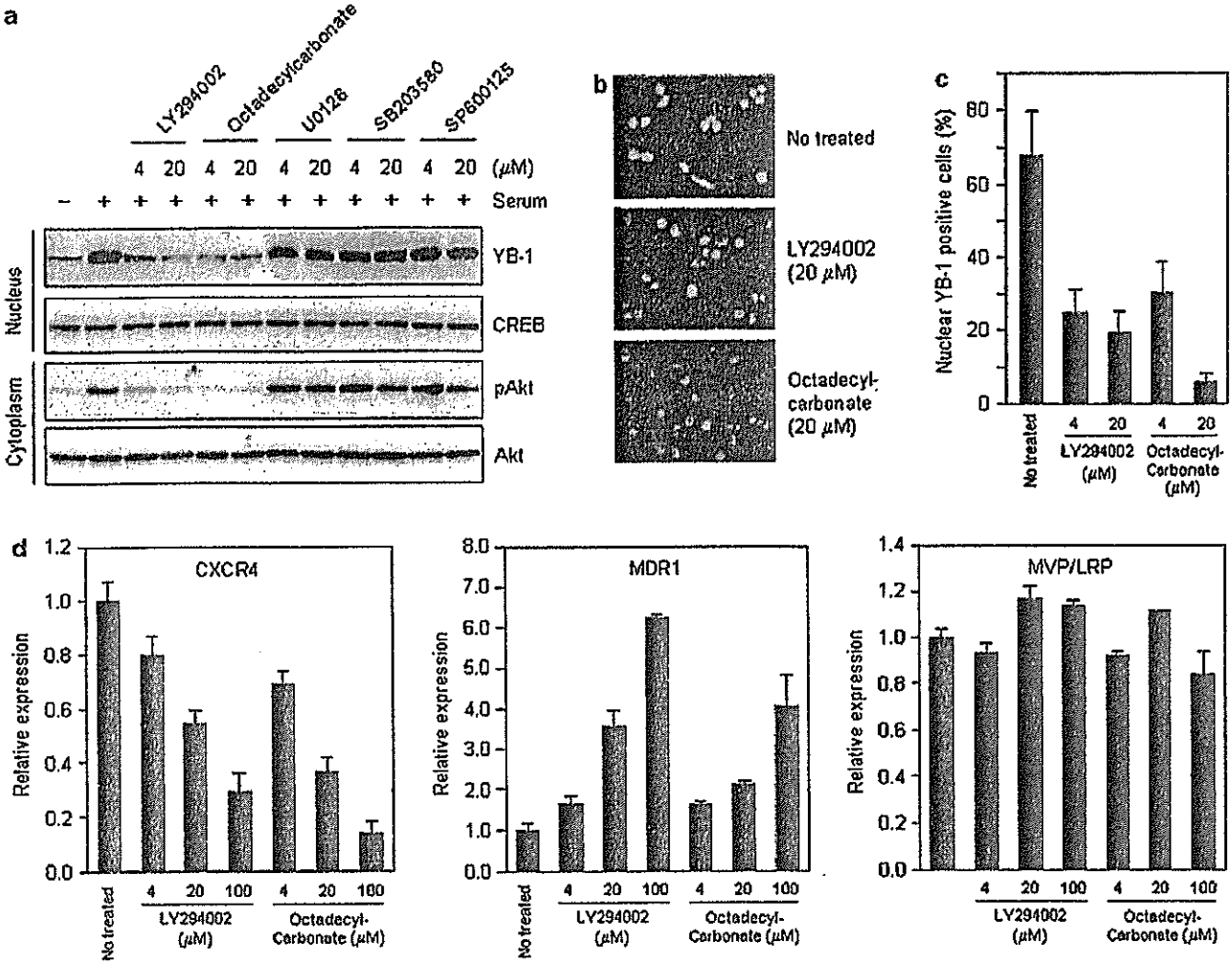

Figure 5 Akt activity is required for YB-1 nuclear accumulation and transcriptional regulation by YB-1. (a) The effect of kinase inhibitors on the nuclear accumulation of YB-1 in SKOV-3 cells. Inhibitors were added 3 h before serum stimulation and nuclear extracts were prepared 1 h after serum stimulation. Anti-YB-1 and anti-CREB immunoblots were performed with nuclear extracts, and anti-pAkt and anti-Akt immunoblots were performed on cytoplasmic extracts. CREB and Akt are shown as a loading control. (b) Immunofluorescent staining for YB-1. SKOV-3 cells were treated with LY294002 or octadecylcarbonate for 24 h and then stained with YB-1. Cells were fixed and permeabilized, incubated at 4°C with the primary YB-1 antibody, then with the Alexa Flour 546-labelled secondary antibody. (c) Quantitative analysis of YB-1 nuclear localization in SKOV-3 cells as shown in Figure 2b. Data are mean of three independent experiments; bars ±s.d. (d) QRT-PCR for MDR1, MVP/LRP, CXCR4 and housekeeping gene GAPDH. The relative gene expression for each sample was determined using the formula $2^{(-\Delta C_t)} = 2^{(C_t(\text{GAPDH})-C_t(\text{target}))}$ which reflected target gene expression normalized to GAPDH levels. Data were mean of three independent experiments; bars ±s.d.

the development of tumor growth, angiogenesis and metastasis not only in ovarian cancer (Scotton *et al.*, 2002) but also in other tumor types including breast cancer (Muller *et al.*, 2001), melanoma (Robledo *et al.*, 2001; Murakami *et al.*, 2002) and prostate cancer (Darash-Yahana *et al.*, 2004). Jiang *et al.* (2006) further demonstrated that CXCR4 expression could be an important prognostic marker for ovarian cancers: the rate of CXCR4 expression in refractory and recurrent group was significantly higher than that in non-recurrent group. Our previous studies showed a significant association of nuclear localization of YB-1 with unfavorable prognosis of patients with ovarian cancers (Kamura *et al.*, 1999; Huang *et al.*, 2004). Clinicopathological analysis whether nuclear expression of YB-1 can be associated with CXCR4 expression or CXCL12 (SDF-1α) in patients with ovarian cancers is now in progress.

Several studies have focused on the role of Akt/PI3K inhibitors as potential tumor suppressor agents. It has been reported that phosphorylation of Akt and mTOR, an Akt substrate, was frequently detected in ovarian cancer (Altomare *et al.*, 2004). In animal model of ovarian cancer, LY294002, a potent inhibitor of Akt activation, could inhibit cancer growth and ascites formation (Hu *et al.*, 2000). Our study also

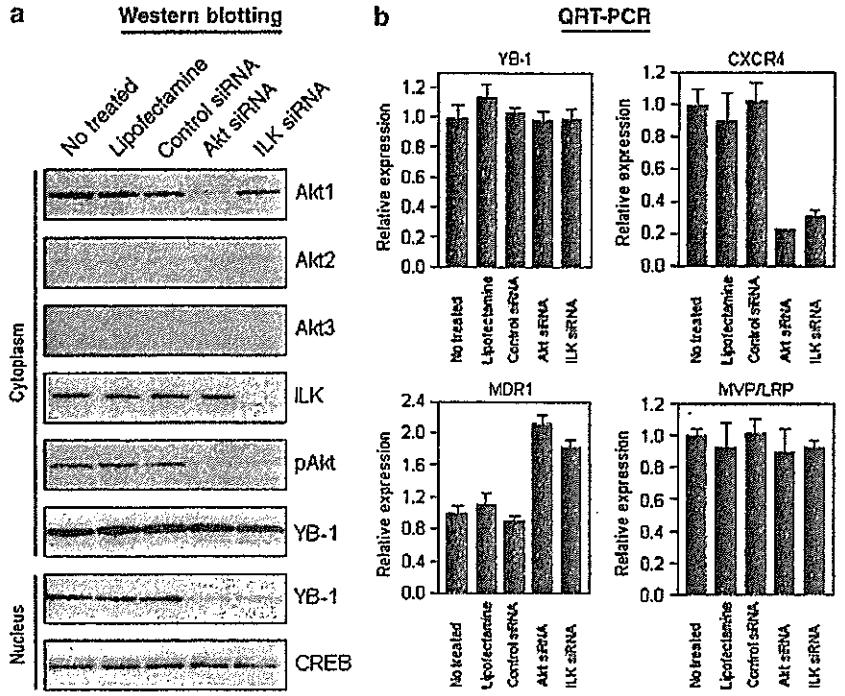

Figure 6 Effect of knock down of Akt and ILK on YB-1 nuclear accumulation, and expression of MDR1, MVP/LRP and CXCR4. (a) SKOV-3 cells were treated with Akt siRNA (100 nM), ILK siRNA (10 nM) or control siRNA (100 nM) for 48 h, and then cytoplasmic and nuclear extracts were prepared. Anti-Akt1, anti-Akt2, anti-Akt3, anti-ILK, anti-pAkt, and anti-YB-1 immunoblots were performed with cytoplasmic extracts, and anti-YB-1 and anti-CREB immunoblots were performed with nuclear extracts. (b) SKOV-3 cells were treated with Akt siRNA (100 nM) or ILK siRNA (10 nM) for 48 h and then total RNA was prepared. QRT-PCR was performed for MDR1, MVP/LRP, CXCR4, YB-1 and GAPDH housekeeping gene. The relative gene expression for each sample was determined using the formula $2^{(-\Delta C_t)} = 2^{(C_t(\text{GAPDH}) - C_t(\text{target}))}$ which reflected target genes normalized to GAPDH levels. Data were mean of three independent experiments; bars ±s.d.

demonstrated that both Akt phosphorylation and YB-1 nuclear localization were blocked by administration of LY294002 in SKOV-3 xenograft model. Nuclear localization of YB-1 is induced through various pathways including Akt (see Introduction). The Akt-dependent pathway for YB-1 nuclear localization would provide further insight how Akt-targeting anticancer therapeutic strategy could be developed.

In conclusion, we have identified several genes that are regulated by YB-1 and/or its nuclear localization. Further immunohistochemical analysis should be required to elucidate the role of YB-1 in the expression of *CXCR4* and other relevant genes that are associated with the clinicopathological characteristics in human ovarian cancers. Based on our present experimental results, we aim to present YB-1 and YB-1-dependent gene networks as molecular targets for the further development of novel anticancer therapeutic strategies.

Materials and methods

Cell culture and reagents

OVCAR-3 and SKOV-3 were purchased from American Type Culture Collection (Manassas, VA, USA). RMG-I, RMG-II, RMG-III, RMBG and RTSG were kindly provided by Dr S Nozawa, Department of Obstetrics and Gynecology, Keio University. These cell lines were grown in DMEM supplemented with 10% fetal bovine serum (FBS) in an atmosphere of 5% CO_2. LY294002 and U0126 were purchased from Sigma Chemical Co. (St Louis, MO, USA). 1L-6-hydroxymethyl-*chiro*-inositol 2(*R*)-2-*O*-methyl-3-*O*-octadecylcarbonate (Hu *et al*., 2000), SB203580 (Cuenda *et al*., 1995), and SP600125 (Bennett *et al*., 2001) were obtained from Calbiochem (San Diego, CA, USA). Anti-YB-1 was generated as described previously (Ohga *et al*., 1996). Anti-CREB, anti-PKB/Akt, anti-phospho-PKB/Akt, anti-ILK, Akt siRNA and ILK siRNA were obtained from Cell Signaling Technology (Beverly, MA, USA).

Western blotting

Western blotting was performed as previously described (Kaneko *et al*., 2004). Cells were lysed in buffer A (10 mM HEPES (pH7.9), 10 mM KCl, 10 mM EDTA, 1 mM DTT, 0.4% v/v IGEPAL, 1 mM Na_3VO_4, 1 mM PMSF, and 10 μg/ml aprotinin and leupeptin) for 10 min on ice, and then centrifuged for 3 min at 15 000 r.p.m. The supernatant fractions (cytoplasmic soluble proteins) were collected. The nuclear pellet was then washed and then lysed in buffer C (20 mM HEPES (pH7.9), 200 mM NaCl, 1 mM EDTA, 5% v/v glycerol, 1 mM DTT, 1 mM Na_3VO_4, 1 mM PMSF and 10 μg/ml aprotinin and leupeptin). Lysates were incubated on ice for 2 h, and then centrifuged 15 000 r.p.m. for 5 min. The lysates were separated by sodium dodecyl sulfate–polyacryl amide gel electrophoresis (SDS–PAGE), and then were transferred to a nitrocellulose membrane. The membrane were incubated with the primary antibody and visualized with secondary antibody coupled to horseradish peroxidase (Cell Signaling Technology)

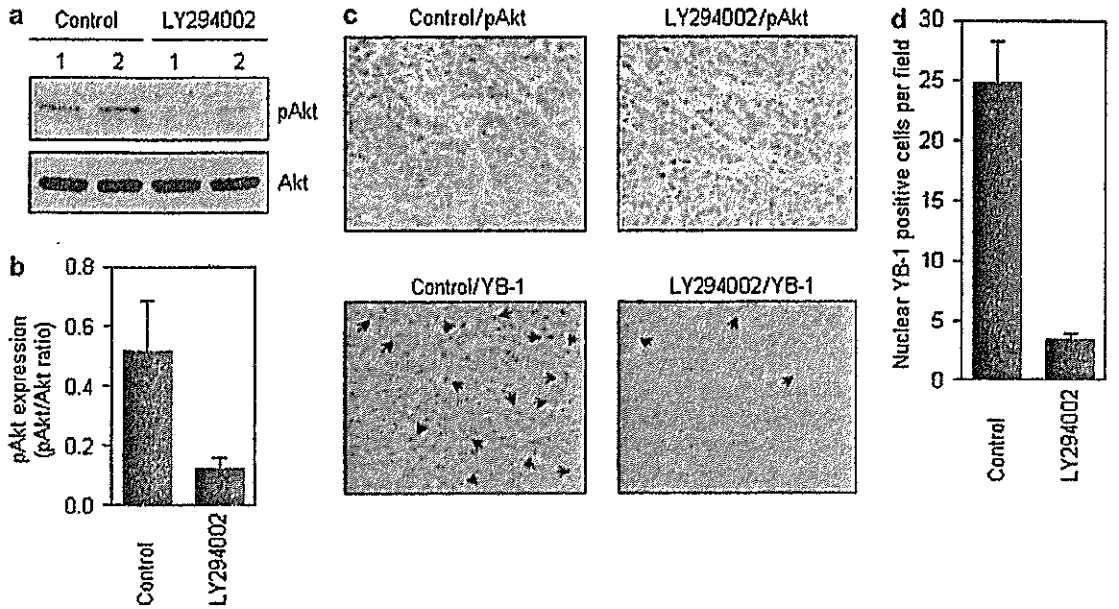

Figure 7 Effect of LY294002 on Akt phosphorylation and YB-1 nuclear localization in SKOV-3 xenograft. (a) Effect of LY294002 on Akt phosphorylation in SKOV-3 xenograft. SKOV-3 cells were injected subcutaneously (5.0×10^6 cells/0.1 ml/mouse). When tumors reached approximately 1000–2000 mm³, animals were randomly assigned to two groups of five. The first group received i.p. injections of DMSO as a control. The second group received i.p. injections of 50 mg/kg LY294002. One hour after LY294002 injection, mice were killed humanely (while anesthetized) by cervical dislocation and tumors were excised. Western blot analysis was carried out using cytosolic extracts prepared from tumor tissues from two animals treated with or without drug. (b) Quantitative analysis of Akt phosphorylation in SKOV-3 tumor xenograft. Levels of Akt phosphorylation were normalized to their nonphosphorylated form as shown in Figure 7a. Data are expressed as mean ± s.d. of three to five mice. (c) Immunohistochemical staining was carried out using conventional protocols. The arrows indicate positive cell nuclei staining for YB-1 (×200 magnification). (d) Quantitative analysis of YB-1 nuclear localization in SKOV-3 tumor xenograft. YB-1 nuclear localization was determined by counting the number of positive YB-1 nuclear cells in high-power fields as shown in Figure 7b. Data were mean of each section (five sections per mouse). Columns, mean; bars ± s.d.

and SuperSignal West Pico Chemiluminescent Substrate (Pierce, Rockford, IL, USA). Bands on Western blots were analysed densitometrically using Scion Image software (version 4.0.2; Scion Corp., Frederick, MD, USA).

Oligonucleotide microarray analysis

The siRNA corresponding to nucleotide sequences of the YB-1 (5′-GGU UCC CAC CUU ACU ACA U-3′) was purchased from QIAGEN Inc. (Valencia, CA, USA). A negative control siRNA was obtained from Invitrogen (Carlsbad, CA, USA). siRNA duplexes were transfected using LipofectAMINE2000 and Opti-MEM medium (Invitrogen) according to the manufacturer's recommendations. Duplicate samples were prepared for microarray hybridization. At 48 h after siRNA transfection, total RNA was extracted from cell cultures using ISOGEN (Nippon Gene Co. Ltd., Tokyo, Japan). Total RNA (2 μg) was reverse-transcribed using GeneChip 3′-Amplification Reagents One-Cycle cDNA Synthesis Kit (Affymetrix Inc., Santa Clara, CA, USA) and then labeled with Cy5 or Cy3. The labeled cRNA was applied to the oligonucleotide microarray (Human Genome U133 Plus 2.0 Array, Affymetrix). The microarray was scanned on a GeneChip Scanner3000 and the image was analysed using a GeneChip Operating Software ver1.

Correlation analysis of gene expression, and clustering of cell lines and genes expression

Gene expression data for the 60 human tumor cell lines were obtained from the Developmental Therapeutics Program (http://www.dtp. nci.nih.gov/), expressed as log of the mRNA levels in cell line/mRNA levels in reference pool in the NCI screen. Pearson correlation coefficients were calculated for each gene–gene pair. Hierarchical clustering can be used to group cell lines and genes in term of their patterns of gene expression. To obtain cluster trees for genes that showed distinct expression patterns across the 60 cell lines, we used the program 'Cluster' and 'Tree View' (http://rana.lbl.gov/) with average linkage clustering and a correlation metric (Eisen *et al.*, 1998).

Quantitative real-time polymerase chain reaction

RNA was reverse transcribed from random hexamers using AMV reverse transcriptase (Promega, Madison, WI, USA). Real-time quantitative PCR was performed using the Real-Time PCR system 7300 (Applied Biosystems, Foster City, CA, USA) as described previously (Maruyama *et al.*, 2006). In brief, the PCR amplification reaction mixtures (20 μl) contained cDNA, primer pairs, the dual-labeled fluorogenic probe, and TaqMan Universal PCR Master Mix (Applied Biosystems). The thermal cycle conditions included maintaining the reactions at 50°C for 2 min and at 95°C for 10 min, and then alternating for 40 cycles between 95°C for 15 s and 60°C for 1 min. The primer pairs and the probe were obtained from Applied Biosystems. The relative gene expression for each sample was determined using the formula $2^{(-\Delta C_t)} = 2^{(C_t(\mathrm{GAPDH}) - C_t(\mathrm{target}))}$ which reflected target gene expression normalized to GAPDH levels.

Immunofluorescence

Cells were plated on glass coverslips in six-well plates and allowed to attach overnight. Then, cells were rinsed with PBS

and then fixed in 4% paraformaldehyde/PBS for 30 min. Cells were rinsed twice with PBS and then permeabilized with 0.5 ml of solution containing 5% BSA, 0.2% Triton X-100 in PBS for 90 min. After 1 h of blocking with 2% goat serum, the cells were incubated overnight with primary antibody at 4°C in 1% BSA in PBS. Cells were then rinsed three times with PBS and incubated with 1 μg/ml of Alexa Flour 546-labeled secondary antibody (Molecular Probe, Eugene, OR, USA) in 1% BSA in PBS for 60 min. Coverslips were mounted on slide glasses using gel mount and viewed using an Olympus BX51 florescence microscope (Tokyo, Japan) and photographed with Olympus DP-70 digital camera.

Tumor xenograft study

Male BALB/c nude mice were obtained from Kyudo Co., Ltd. (Fukuoka, Japan). SKOV-3 cells were harvested and resuspended in PBS. The suspension was injected subcutaneously in the mice (5.0×10^6 cells/0.1 ml/mouse). When tumors reached about 1000–2000 mm^3, animals were randomly assigned to two groups of five mice each. The first group received i.p. injections of DMSO as control. The second group received i.p. injection of LY294002 at 50 mg/kg. At 1 h after LY294002 injection, mice were killed humanly (mice still anesthetized) by cervical dislocation and tumors were excised. For immunohistchemistry, one part of the tumor tissue was fixed in formalin and embed in paraffin.

Acknowledgements

We thank Y Yamada and Y Yamasaki in Hanno Research Center of Taiho Pharmaceutical Co. Ltd. for fruitful discussion, and N Shinbaru in Kyushu University for editorial help. This study was supported by the COE program for Medical Sciences, Kurume University, and grant-in-aid for scientific research on priority areas cancer from Ministry of Education Culture, Sports Science, and Technology of Japan and the 2nd-Comprehensive Ten-Year Strategy for Cancer Control from the Ministry of Health, Welfare and Labor, Japan.

References

Altomare DA, Wang HQ, Skele KL, De Rienzo A, Klein-Szanto AJ, Godwin AK *et al.* (2004). AKT and mTOR phosphorylation is frequently detected in ovarian cancer and can be targeted to disrupt ovarian tumor cell growth. *Oncogene* **23**: 5853–5857.

Asakuno K, Kohno K, Uchiumi T, Kubo T, Sato S, Isono M *et al.* (1994). Involvement of a DNA binding protein, MDR-NF1/YB-1, in human MDR1 gene expression by actinomycin D. *Biochem Biophys Res Commun* **199**: 1428–1435.

Ashizuka M, Fukuda T, Nakamura T, Shirasuna K, Iwai K, Izumi H *et al.* (2002). Novel translational control through an iron-responsive element by interaction of multifunctional protein YB-1 and IRP2. *Mol Cell Biol* **22**: 6375–6383.

Bargou RC, Jurchott K, Wagener C, Bergmann S, Metzner S, Bommert K *et al.* (1997). Nuclear localization and increased levels of transcription factor YB-1 in primary human breast cancers are associated with intrinsic MDR1 gene expression. *Nat Med* **3**: 447–450.

Bennett BL, Sasaki DT, Murray BW, O'Leary EC, Sakata ST, Xu W *et al.* (2001). SP600125, an anthrapyrazolone inhibitor of Jun N-terminal kinase. *Proc Natl Acad Sci USA* **98**: 13681–13686.

Caruz A, Samsom M, Alonso JM, Alcami J, Baleux F, Virelizier JL *et al.* (1998). Genomic organization and promoter characterization of human CXCR4 gene. *FEBS Lett* **426**: 271–278.

Cuenda A, Rouse J, Doza YN, Meier R, Cohen P, Gallagher TF *et al.* (1995). SB 203580 is a specific inhibitor of a MAP kinase homologue which is stimulated by cellular stresses and interleukin-1. *FEBS Lett* **364**: 229–233.

Darash-Yahana M, Pikarsky E, Abramovitch R, Zeira E, Pal B, Karplus R *et al.* (2004). Role of high expression levels of CXCR4 in tumor growth, vascularization, and metastasis. *FASEB J* **18**: 1240–1242.

Dooley S, Said HM, Gressner AM, Floege J, En-Nia A, Mertens PR. (2006). Y-box protein-1 is the crucial mediator of antifibrotic interferon-gamma effects. *J Biol Chem* **281**: 1784–1795.

Eisen MB, Spellman PT, Brown PO, Botstein D. (1998). Cluster analysis and display of genome-wide expression patterns. *Proc Natl Acad Sci USA* **95**: 14863–14868.

En-Nia A, Yilmaz E, Klinge U, Lovett DH, Stefanidis I, Mertens PR. (2005). Transcription factor YB-1 mediates DNA polymerase alpha gene expression. *J Biol Chem* **280**: 702–711.

Evdokimova V, Ruzanov P, Imataka H, Raught B, Svitkin Y, Ovchinnikov LP *et al.* (2001). The major mRNA-associated protein YB-1 is a potent 5′ cap-dependent mRNA stabilizer. *EMBO J* **20**: 5491–5502.

Fukuda T, Ashizuka M, Nakamura T, Shibahara K, Maeda K, Izumi H *et al.* (2004). Characterization of the 5′-untranslated region of YB-1 mRNA and autoregulation of translation by YB-1 protein. *Nucleic Acids Res* **32**: 611–622.

Furukawa M, Uchiumi T, Nomoto M, Takano H, Morimoto RI, Naito S *et al.* (1998). The role of an inverted CCAAT element in transcriptional activation of the human DNA topoisomerase IIalpha gene by heat shock. *J Biol Chem* **273**: 10550–10555.

Holm PS, Bergmann S, Jurchott K, Lage H, Brand K, Ladhoff A *et al.* (2002). YB-1 relocates to the nucleus in adenovirus-infected cells and facilitates viral replication by inducing E2 gene expression through the E2 late promoter. *J Biol Chem* **277**: 10427–10434.

Hu L, Zaloudek C, Mills GB, Gray J, Jaffe RB. (2000). *In vivo* and *in vitro* ovarian carcinoma growth inhibition by a phosphatidylinositol 3-kinase inhibitor (LY294002). *Clin Cancer Res* **6**: 880–886.

Huang X, Ushijima K, Komai K, Takemoto Y, Motoshima S, Kamura T *et al.* (2004). Co-expression of Y box-binding protein-1 and P-glycoprotein as a prognostic marker for survival in epithelial ovarian cancer. *Gynecol Oncol* **93**: 287–291.

Ise T, Nagatani G, Imamura T, Kato K, Takano H, Nomoto M *et al.* (1999). Transcription factor Y-box binding protein 1 binds preferentially to cisplatin-modified DNA and interacts with proliferating cell nuclear antigen. *Cancer Res* **59**: 342–346.

Jiang YP, Wu XH, Shi B, Wu WX, Yin GR. (2006). Expression of chemokine CXCL12 and its receptor CXCR4 in human epithelial ovarian cancer: an independent prognostic factor for tumor progression. *Gynecol Oncol* **103**: 226–233.

Kamura T, Yahata H, Amada S, Ogawa S, Sonoda T, Kobayashi H *et al.* (1999). Is nuclear expression of Y box-binding protein-1 a new prognostic factor in ovarian serous adenocarcinoma? *Cancer* **85**: 2450–2454.

Kaneko Y, Kitazato K, Basaki Y. (2004). Integrin-linked kinase regulates vascular morphogenesis induced by vascular endothelial growth factor. *J Cell Sci* **117**: 407–415.

Kohno K, Izumi H, Uchiumi T, Ashizuka M, Kuwano M. (2003). The pleiotropic functions of the Y-box-binding protein, YB-1. *Bioessays* **25**: 691–698.

Koike K, Uchiumi T, Ohga T, Toh S, Wada M, Kohno K *et al.* (1997). Nuclear translocation of the Y-box binding protein by ultraviolet irradiation. *FEBS Lett* **417**: 390–394.

Kryczek I, Lange A, Mottram P, Alvarez X, Cheng P, Hogan M *et al.* (2005). CXCL12 and vascular endothelial growth factor synergistically induce neoangiogenesis in human ovarian cancers. *Cancer Res* **65**: 465–472.

Kuwano M, Oda Y, Izumi H, Yang SJ, Uchiumi T, Iwamoto Y *et al.* (2004). The role of nuclear Y-box binding protein 1 as a global marker in drug resistance. *Mol Cancer Ther* **3**: 1485–1492.

Ladomery M, Sommerville J. (1995). A role for Y-box proteins in cell proliferation. *Bioessays* **17**: 9–11.

Maruyama Y, Ono M, Kawahara A, Yokoyama T, Basaki Y, Kage M *et al.* (2006). Tumor growth suppression in pancreatic cancer by a putative metastasis suppressor gene Cap43/NDRG1/Drg-1 through modulation of angiogenesis. *Cancer Res* **66**: 6233–6242.

Matsumoto K, Wolffe AP. (1998). Gene regulation by Y-box proteins: coupling control of transcription and translation. *Trends Cell Biol* **8**: 318–323.

Mossink MH, van Zon A, Scheper RJ, Sonneveld P, Wiemer EA. (2003). Vaults: a ribonucleoprotein particle involved in drug resistance? *Oncogene* **22**: 7458–7467.

Muller A, Homey B, Soto H, Ge N, Catron D, Buchanan ME *et al.* (2001). Involvement of chemokine receptors in breast cancer metastasis. *Nature* **410**: 50–56.

Murakami T, Maki W, Cardones AR, Fang H, Tun Kyi A, Nestle FO *et al.* (2002). Expression of CXC chemokine receptor-4 enhances the pulmonary metastatic potential of murine B16 melanoma cells. *Cancer Res* **62**: 7328–7334.

Ohga T, Koike K, Ono M, Makino Y, Itagaki Y, Tanimoto M *et al.* (1996). Role of the human Y box-binding protein YB-1 in cellular sensitivity to the DNA-damaging agents cisplatin, mitomycin C, and ultraviolet light. *Cancer Res* **56**: 4224–4228.

Ohga T, Uchiumi T, Makino Y, Koike K, Wada M, Kuwano M *et al.* (1998). Direct involvement of the Y-box binding protein YB-1 in genotoxic stress-induced activation of the human multidrug resistance 1 gene. *J Biol Chem* **273**: 5997–6000.

Porcile C, Bajetto A, Barbieri F, Barbero S, Bonavia R, Biglieri M *et al.* (2005). Stromal cell-derived factor-1alpha (SDF-1alpha/CXCL12) stimulates ovarian cancer cell growth through the EGF receptor transactivation. *Exp Cell Res* **308**: 241–253.

Robledo MM, Bartolome RA, Longo N, Rodriguez-Frade JM, Mellado M, Longo I *et al.* (2001). Expression of functional chemokine receptors CXCR3 and CXCR4 on human melanoma cells. *J Biol Chem* **276**: 45098–45105.

Scotton CJ, Wilson JL, Milliken D, Stamp G, Balkwill FR. (2001). Epithelial cancer cell migration: a role for chemokine receptors? *Cancer Res* **61**: 4961–4965.

Scotton CJ, Wilson JL, Scott K, Stamp G, Wilbanks GD, Fricker S *et al.* (2002). Multiple actions of the chemokine CXCL12 on epithelial tumor cells in human ovarian cancer. *Cancer Res* **62**: 5930–5938.

Sorokin AV, Selyutina AA, Skabkin MA, Guryanov SG, Nazimov IV, Richard C *et al.* (2005). Proteasome-mediated cleavage of the Y-box-binding protein 1 is linked to DNA-damage stress response. *EMBO J* **24**: 3602–3612.

Stein U, Bergmann S, Scheffer GL, Scheper RJ, Royer HD, Schlag PM *et al.* (2005). YB-1 facilitates basal and 5-fluorouracil-inducible expression of the human major vault protein (MVP) gene. *Oncogene* **24**: 3606–3618.

Stein U, Jurchott K, Walther W, Bergmann S, Schlag PM, Royer HD. (2001). Hyperthermia-induced nuclear translocation of transcription factor YB-1 leads to enhanced expression of multidrug resistance-related ABC transporters. *J Biol Chem* **276**: 28562–28569.

Stenina OI, Poptic EJ, DiCorleto PE. (2000). Thrombin activates a Y box-binding protein (DNA-binding protein B) in endothelial cells. *J Clin Invest* **106**: 579–587.

Sutherland BW, Kucab J, Wu J, Lee C, Cheang MC, Yorida E *et al.* (2005). Akt phosphorylates the Y-box binding protein 1 at Ser102 located in the cold shock domain and affects the anchorage-independent growth of breast cancer cells. *Oncogene* **24**: 4281–4292.

Supplementary Information accompanies the paper on the Oncogene website (http://www.nature.com/onc).

Cancer Chemother Pharmacol
DOI 10.1007/s00280-006-0314-6

EGFR mutation in various tissues

Kazuto Nishio · Tokuzo Arao · Terufumi Kato · Hideyuki Yokote

© Springer-Verlag 2006

Abstract Somatic mutations have been demonstrated in various tumors. *EGFR* mutations were first demonstrated in adenocarcinoma of the lung, and a large-scale retrospective study has clearly shown that these mutations are specifically observed in this form of the disease. Recently, possible occurrence of *EGFR* mutations in other tumor types including ovarian and colorectal malignancies has been reported. This raises the possibility of application of EGFR-specific tyrosine kinase inhibitors (EGFR-TKI) to the treatment of these malignancies, although broad success in this venture would depend on the frequency of such mutations. In this article, we discuss somatic mutations in various tumors as well as potential application of TKI to their treatment. Ethnic difference in the frequency of somatic mutations is another area of interest since it is closely related to clinical response to EGFR-TKIs. Preliminary studies have revealed such ethnic variations regarding *EGFR* mutation and gene amplification. Ethnic difference of transcriptional regulation of *EGFR* has also been demonstrated. We recently found a biomarker related to clinical response to EGFR-TKI that might explain the ethnic differences in response to this therapy. Various tyrosine kinases are known targets of TKIs. Thus genomics of individual patients may allow personalized target-based therapeutics.

Keywords EGFR mutation · Tyrosine kinase inhibitor · Ethnicity · HLA

This work was presented at the 21st Bristol-Myers Squibb Nagoya International Cancer Treatment Symposium, "Lung Cancer: Novel Therapy against Malfunctioning Molecules", 24–25 February 2006, Nagoya, Japan.

K. Nishio (✉) · T. Arao · T. Kato · H. Yokote
Pharmacology Division, National Cancer Center Research Institute, Tsukiji 5-1-1, Chuo-ku, Tokyo 104-0045, Japan
e-mail: knishio@med.kindai.ac.jp

K. Nishio · T. Arao · H. Yokote
Department of Genome Biology,
Kinki University School of Medicine, Osaka, Japan

EGFR mutation in various cancers

Somatic mutations have been demonstrated in various tumors. *EGFR* mutations were first demonstrated in adenocarcinoma of the lung, and a large-scale retrospective study has clearly shown that these mutations are specifically observed in this form of the disease [10]. However, extensive analysis of somatic mutation in various tumors subsequently demonstrated the existence of *EGFR* somatic mutation in many human tumors such as colorectal and head and neck cancer, renal cell carcinoma, prostate cancer, and cholangiocarcinoma [4, 7, 8]. Gwak et al. [5] reported *EGFR* mutation in cholangiocarcinoma and found that it was detectable in 13.6% (3/22) of patients. The type of mutation was deletion of exon 19. This is commonly observed in intrahepatic and poorly differentiated tumors. These and other researchers also reported this *EGFR* mutation in squamous cell head and neck carcinoma [7], and Cohen's group demonstrated a new mutation on *erb2* and gene amplification in this disease [3]. The mutation has also been reported in persistent ovarian and primary peritoneal carcinoma in clinical phase II trials of gefitinib [14]. Similar types of mutation have been reported in lung cancers, although these seem to be of minor occurrence [4]. Thus somatic mutations of *EGFR* exist in various tumors. Because of limited samples, it

remains unknown whether *EGFR* mutation in cancer is correlated with clinical response to EGFR-specific tyrosine kinase inhibitors (EGFR-TKI). *EGFR* mutation in other types of tumors than lung cancer seems correlated with immunohistochemical expression but correlation with gene amplification is unknown [14]. Functional aspects of *EGFR* mutation in other types of tumors are also only partially understood. To clarify the significance of somatic mutations in various tumors, tissue banking is necessary. In addition, validated and standardized analytical methods and cross-validation are important to give consistent results. We should also consider how to conduct clinical trials of target-based drugs for less common tumors based on biological data.

Ethnic difference in *EGFR* mutation

Ethnic difference in *EGFR* mutation is another important topic. It is considered that ethnic differences may determine both the frequency of *EGFR* mutation and response to TKi [2]. However, although it has not been fully discussed whether these differences are due to ethnic or merely geographical divides, ethnicity can explain differences in clinical response because of the data acquired in Asian–US patients. It is also considered that differences among the regions of Asia might be obtained: patterns of *EGFR* mutation may differ between Japanese, Chinese, Korean, South Indian, and Turkish individuals [16]. Expanding genome databases should eventually pinpoint the contribution of ethnicity in this regard. Already there is some evidence related to ethnic differences. A CA repeat exists in exon 1 of *EGFR*, related to transcriptional level of this gene. The length of CA repeat varies and is related to ethnicity [9]. Japanese have longer CA repeat compared with Caucasians. Moreover, intron 1 polymorphism reportedly mediates response to EGFR-TKI [1].

What are the differences among the types of *EGFR* mutation? The deletion mutation in exon 19 and point mutation L858R in exon 21 are the two major mutations. Previously, we speculated that the deletion mutation is more frequently detected in Japanese and Asian lung cancer patients as compared with Caucasians. However, recent data seem to refute ethnic difference in the types of *EGFR* mutations [12].

A predictive biomarker related to ethnic difference of sensitivity to gefitinib

Ethnic difference might also exist in sensitivity to drugs. In most such cases, gene polymorphism including microsatellite polymorphism and single nucleotide polymorphism may explain ethnic difference of response to drugs.

Using microarray technique, we analyzed gene expression profiles of peripheral mononuclear cells in lung cancer patients receiving gefitinib as a first-line monotherapy. Our results revealed that HLA genotype was closely related to response to this agent. On the other hand, large ethnic difference of HLA genotype was recognized. Previous reports have demonstrated that HLA genotype plays a role in the metabolism of certain drugs and may be a prognostic factor in malignancies such as gastric, ovarian, and cervical cancers [6, 11, 13, 15, 17]. We hypothesize that HLA subtype may be related to response to gefitinib and might explain ethnic differences. Cross-validation study of this HLA biomarker is ongoing.

Ethnic difference of gefitinib toxicity profile

Subpopulation analysis of gefitinib's toxicity in the ISEL study revealed that only southwest Asian and Taiwanese patients exhibited high ratios of interstitial lung disease (ILD) while on this therapy [16]. However, ILD might not have been induced by gefitinib. More interestingly, the data indicated that Indian–British patients experienced severe (grade 3) skin toxicity along with higher response to gefitinib. Although these phenomena are based on subpopulation analysis, we can speculate that ethnic difference might guide toxicity as well as clinical response to EGFR-TKI. Genomic and biomarker research is necessary to further elucidate these preliminary findings.

Acknowledgment We thank Dr. N. Thatcher (Christie Hosp NHS Trust) for personal communication with T. Kato.

References

1. Amador ML, Oppenheimer D, Perea S, Maitra A, Cusati G, Iacobuzio-Donahue C, Baker SD, Ashfaq R, Takimoto C, Forastiere A, Hidalgo M (2004) An epidermal growth factor receptor intron 1 polymorphism mediates response to epidermal growth factor receptor inhibitors. Cancer Res 64:9139–9143
2. Calvo E, Baselga J (2006) Ethnic differences in response to epidermal growth factor receptor tyrosine kinase inhibitors. J Clin Oncol 24:2158–2163
3. Cohen EE, Lingen MW, Martin LE, Harris PL, Brannigan BW, Haserlat SM, Okimoto RA, Sgroi DC, Dahiya S, Muir B, Clark JR, Rocco JW, Vokes EE, Haber DA, Bell DW (2005) Response of some head and neck cancers to epidermal growth factor receptor tyrosine kinase inhibitors may be linked to mutation of *ERBB2* rather than *EGFR*. Clin Cancer Res 11:8105–8108

4. Douglas DA, Zhong H, Ro JY, Oddoux C, Berger AD, Pincus MR, Satagopan JM, Gerald WL, Scher HI, Lee P, Osman I (2006) Novel mutations of epidermal growth factor receptor in localized prostate cancer. Front Biosci 11:2518–2525
5. Gwak GY, Yoon JH, Shin CM, Ahn YJ, Chung JK, Kim YA, Kim TY, Lee HS (2005) Detection of response-predicting mutations in the kinase domain of the epidermal growth factor receptor gene in cholangiocarcinomas. J Cancer Res Clin Oncol 131:649–652
6. Klein B, Klein T, Nyska A, Shapira J, Figer A, Schwartz A, Rakovsky E, Livni E, Lurie H (1991) Expression of HLA class I and class II in gastric carcinoma in relation to pathologic stage. Tumour Biol 12:68–74
7. Lee JW, Soung YH, Kim SY, Nam HK, Park WS, Nam SW, Kim MS, Sun DI, Lee YS, Jang JJ, Lee JY, Yoo NJ, Lee SH (2005) Somatic mutations of *EGFR* gene in squamous cell carcinoma of the head and neck. Clin Cancer Res 11:2879–2882
8. Lee SC, Lim SG, Soo R, Hsieh WS, Guo JY, Putti T, Tao Q, Soong R, Goh BC (2006) Lack of somatic mutations in *EGFR* tyrosine kinase domain in hepatocellular and nasopharyngeal carcinoma. Pharmacogenet Genomics 16:73–74
9. Liu W, Innocenti F, Chen P, Das S, Cook EH Jr, Ratain MJ (2003) Interethnic difference in the allelic distribution of human epidermal growth factor receptor intron 1 polymorphism. Clin Cancer Res 9:1009–1012
10. Lynch TJ, Bell DW, Sordella R, Gurubhagavatula S, Okimoto RA, Brannigan BW, Harris PL, Haserlat SM, Supko JG, Haluska FG, Louis DN, Christiani DC, Settleman J, Haber DA (2004) Activating mutations in the epidermal growth factor receptor underlying responsiveness of non-small-cell lung cancer to gefitinib. N Engl J Med 350:2129–2139
11. Ogoshi K, Tajima T, Mitomi T, Makuuchi H, Tsuji K (1997) HLA-A2 antigen status predicts metastasis and response to immunotherapy in gastric cancer. Cancer Immunol Immunother 45:53–59
12. Riely GJ, Pao W, Pham D, Li AR, Rizvi N, Venkatraman ES, Zakowski MF, Kris MG, Ladanyi M, Miller VA (2006) Clinical course of patients with non-small cell lung cancer and epidermal growth factor receptor exon 19 and exon 21 mutations treated with gefitinib or erlotinib. Clin Cancer Res 12:839–844
13. Ryu KS, Lee YS, Kim BK, Park YG, Kim YW, Hur SY, Kim TE, Kim IK, Kim JW (2001) Alterations of HLA class I and II antigen expression in preinvasive, invasive and metastatic cervical cancers. Exp Mol Med 33:136–144
14. Schilder RJ, Sill MW, Chen X, Darcy KM, Decesare SL, Lewandowski G, Lee RB, Arciero CA, Wu H, Godwin AK (2005) Phase II study of gefitinib in patients with relapsed or persistent ovarian or primary peritoneal carcinoma and evaluation of epidermal growth factor receptor mutations and immunohistochemical expression: a gynecologic oncology group study. Clin Cancer Res 11:5539–5548
15. Shen YQ, Zhang JQ, Miao FQ, Zhang JM, Jiang Q, Chen H, Shan XN, Xie W (2005) Relationship between the downregulation of HLA class I antigen and clinicopathological significance in gastric cancer. World J Gastroenterol 11:3628–3631
16. Thatcher N, Chang A, Parikh P, Rodrigues Pereira J, Ciuleanu T, von Pawel J, Thongprasert S, Tan EH, Pemberton K, Archer V, Carroll K (2005) Gefitinib plus best supportive care in previously treated patients with refractory advanced non-small-cell lung cancer: results from a randomised, placebo-controlled, multicentre study (Iressa survival evaluation in lung cancer). Lancet 366:1527–1537
17. Vitale M, Pelusi G, Taroni B, Gobbi G, Micheloni C, Rezzani R, Donato F, Wang X, Ferrone S (2005) HLA class I antigen down-regulation in primary ovary carcinoma lesions: association with disease stage. Clin Cancer Res 11:67–72

A Photon Counting Technique for Quantitatively Evaluating Progression of Peritoneal Tumor Dissemination

Kazuyoshi Yanagihara,[1] Misato Takigahira,[1] Fumitaka Takeshita,[2] Teruo Komatsu,[1] Kazuto Nishio,[3] Fumio Hasegawa,[4] and Takahiro Ochiya[2]

[1]Central Animal Laboratory, [2]Section for Studies on Metastasis, [3]Pharmacology Division, and [4]Central RI Laboratory, National Cancer Center Research Institute, Tokyo, Japan

Abstract

We recently established a mouse model of peritoneal dissemination of human gastric carcinoma, including the formation of ascites, by orthotopic transplantation of cultured gastric carcinoma cells. To clarify the processes of expansion of the tumors in this model, nude mice were sacrificed and autopsied at different points of time after the orthotopic transplantation of the cancer cells for macroscopic and histopathologic examination of the tumors. The cancer cells grew actively in the gastric submucosa and invaded the deeper layers to reach the serosal plane. The tumor cells then underwent exfoliation and became free followed by the formation of metastatic lesions initially in the greater omentum and subsequent colonization and proliferation of the tumors on the peritoneum. Although this model allowed the detection of even minute metastases, it was not satisfactory from the viewpoint of quantitative and objective evaluation. To resolve these problems, we introduced a luciferase gene into this tumor cell line with a high metastasizing potential and carried out *in vivo* photon counting analysis. This photon counting technique was found to allow objective and quantitative evaluation of the progression of peritoneal dissemination on a real-time basis. This animal metastatic model is useful for monitoring the responses of tumors to anticancer agents. (Cancer Res 2006; 66(15): 7532-9)

Introduction

Tumor dissemination and ascites are the two major features of cancerous peritonitis. Of the various manifestations of the progression of cancer affecting the i.p. organs (gastric, hepatic, ovarian, and other cancers), cancerous peritonitis is the most closely associated with poor operative results (1–6). In particular, scirrhous gastric cancer (diffusely infiltrative carcinoma or Borrmann's type IV carcinoma or the linitis plastica type) is a high-grade gastric cancer that is difficult to detect in the early stages and is often complicated by peritoneal dissemination (7–9). Although peritoneal dissemination is an important subject, very few experimental studies have been conducted to characterize its occurrence. In general, most of the experimental models of peritoneal dissemination from gastric cancer established to date have involved direct i.p. implantation of cancer cells (10–12). Although these conventional models may allow limited examination of the later stages of peritoneal dissemination, they cannot be expected to allow reasonable evaluation of its early stages. It is well known that implanting human tumor fragments and tumor cells orthotopically into the corresponding organs of nude mice results in much higher metastatic rates (13, 14). However, only one orthotopic implantation model, scirrhous carcinoma of the stomach, has been reported (15). We recently established two scirrhous gastric carcinoma-derived tumor cell lines capable of spontaneous metastasis following ectopic implantation (16). We repeated cycles of orthotopic transplantation of these tumor cell lines, collected cancer cells from the ascitic fluid formed as a result of cancerous peritonitis, and used the collected cells for further cycles of orthotopic transplantation. In this way, we isolated cell lines (44As3, 58As1, and 58As9) with high metastasizing potential and stable metastatic characteristics (17). When these cells were implanted orthotopically into the animals, bloody ascites formed within 3 to 5 weeks, resulting in the death of the animals.

As stated above, conventionally, progression of peritoneal dissemination has been analyzed by implanting cancer cells directly into the peritoneal cavity followed by sacrifice and autopsy of the animals at certain points of time after implantation and, finally, measurement of the number and weight of the tumor nodules in the sacrificed animals (18–20). Evaluation of the efficacy of anticancer agents was also hampered by this limitation (21–25). Evaluation using these methods may be affected by subjective factors and, therefore, unsatisfactory from the viewpoint of quantitative or objective evaluation. In order for our animal model of peritoneal dissemination to be applied universally as a drug evaluation system, we needed to establish a method for quantitative observation and objective evaluation of the relevant variables.

Recent progress in the optical imaging of cancers in animal models presents many potential advantages for recreating the disease process, disease detection, screening, diagnosis, drug development, and treatment evaluation. Fluorescence-based imaging (26–35) and photon counting analysis (36–43) modalities are well developed and allow specific, highly sensitive and quantitative measurements of a wide range of tumor-related variables in mice. Herein, we have shown that photon counting technique is an effective technology in living mice.

Materials and Methods

Established highly metastatic cell lines and culture. 44As3, highly peritoneal metastatic cell line, and parent HSC-44PE, human scirrhous gastric carcinoma-derived cell line, were previously reported (16, 17). When the subclones isolated by repeated s.c. injection of HSC-44PE cells were implanted orthotopically, they spread to the greater omentum, mesenterium, etc. and caused the formation of bloody ascites in a few animals (16). We repeated cycles of isolation of ascitic tumor cells and orthotopic inoculation of these cells, in turn, into animals to isolate highly metastatic

Requests for reprints: Kazuyoshi Yanagihara, Central Animal Laboratory, National Cancer Center Research Institute, 5-1-1 Tsukiji, Chuo-ku, Tokyo 104-0045, Japan. Phone: 81-3-3542-2548; Fax: 81-3-3542-2548; E-mail: kyanagih@gan2.res.ncc.go.jp.

©2006 American Association for Cancer Research.

doi:10.1158/0008-5472.CAN-05-3259

44As3 cell lines, having a strong capability of inducing the formation of ascites (17).

The cell lines were maintained in RPMI 1640 supplemented with 10% FCS (Sigma Chemical, St. Louis, MO), 100 IU/mL penicillin G sodium, and 100 mg/mL streptomycin sulfate (Immuno-Biological Laboratories, Takasaki, Japan) in a 5% CO_2 and 95% air atmosphere at 37°C (17).

***In vivo* photon counting analysis.** 44As3 and HSC-44PE cells were transfected with a complex of 4 μg pEGF-PLuc plasmid DNA (Clontech, Palo Alto, CA) and 24 μL GeneJammer reagent (Stratagene, Cloning Systems, La Jolla, CA) in accordance with the manufacturer's instructions. Stable transfectants were selected in geneticin (400 μg/mL; Invitrogen, Carlsbad, CA), and bioluminescence was used to screen transfected clones for luciferase gene expression using the IVIS system (Xenogen, Alameda, CA). Clones expressing the luciferase gene were named 44As3Luc and HSC44Luc.

Orthotopic implantation of 1×10^6 44As3Luc and HSC44Luc cells was conducted in 6-week-old female BALB/c-*nu/nu* mice (day 0) as described previously (17). *In vivo* photon counting analysis was conducted on a cryogenically cooled IVIS system using Living Image acquisition and analysis software (Xenogen) as described previously (39).

Animal protocols were approved by the committee for Ethics of Animal Experimentation and were in accordance with the Guideline for Animal Experiments in the National Cancer Center. Mice were purchased from CLEA Japan (Tokyo, Japan). The mice were maintained under specific pathogen-free conditions and provided with sterile food, water, and cages. Ambient light was controlled to provide regular cycles of 12 hours of light and 12 hours of darkness.

Therapeutic study with irinotecan (CPT-11). The experimental mice were divided into a control group that received vehicle alone (saline) and experimental groups that received i.v. inoculation of 200 mg/kg/mouse of CPT-11, a clinically active topoisomerase I inhibitor, a level that has been reported to be highly effective in tumor growth (17). On days 3, 7, and 11, tumor-bearing mice received an i.v. injection of CPT-11. The additional injection of CPT-11 was done on days 28, 31, and 35. CPT-11 was purchased from Yakult Honsha (Tokyo, Japan) and dissolved in saline before being injected.

Statistical analysis. All data were analyzed by using the unpaired *t* test and expressed as the mean ± SE. A $P < 0.05$ was considered statistically significant.

Results

Animal model of peritoneal dissemination. The highly metastatic peritoneal cell line used in this study (44As3) was isolated by repeated cycles of orthotopic implantation of HSC-44PE cells and collection of the ascitic tumor cells as described in Materials and Methods (16, 17). As shown in Table 1 and Fig. 1, the tumor formed by this cell line was characterized by a propensity for early peritoneal dissemination and was frequently associated with the formation of ascites and the animals became moribund ~35 days after implantation. On the other hand, the graft cell survival after implantation of the parent cell line (HSC-44PE) was 67% and moribund animals were not seen until ~90 days after implantation, although no ascites formation was observed.

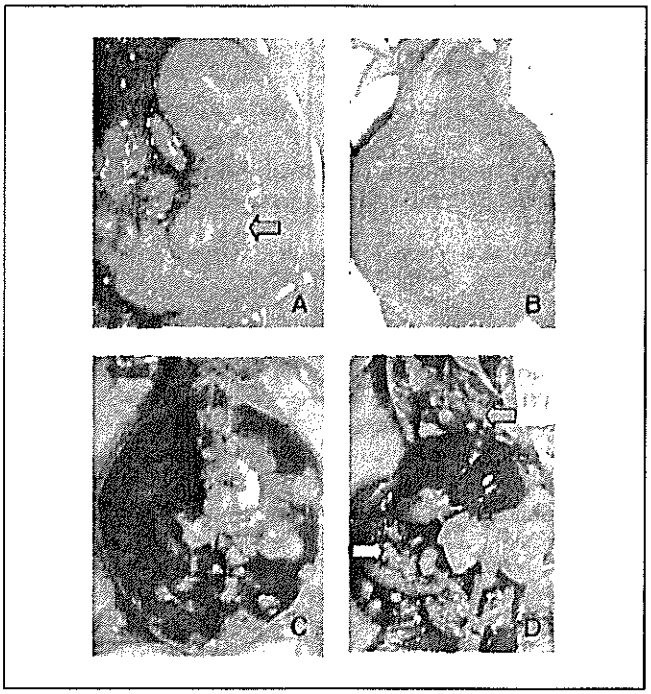

Figure 1. Macroscopic appearance of the peritoneal disseminations after orthotopic implantation of 44As3 cells. *A, green arrow,* orthotopic implantation of the cells in the stomach of nude mice was followed by tumor formation 3 weeks later. *B* and *C,* carcinomatous peritonitis was observed 5 weeks after orthotopic implantation of the cells. Abdominal distension because of bloody ascites was evident. *D,* peritoneal dissemination was recognized from the innumerable whitish nodules visualized in the abdominal cavity, mesenterium (*yellow arrow*), omentum, parietal peritoneum, and diaphragm (*green arrow*).

Anatomic, histopathologic, and ultrastructural analysis of the progression of peritoneal dissemination. To analyze the process of progression of peritoneal dissemination, 44As3 cells (1×10^6) were implanted orthotopically into the gastric wall of nude mice. Every 7 days after transplantation, five animals were

Table 1. Comparison of the survival and metastatic behavior of animals following orthotopic implantation of the highly metastatic and the parent cell lines

Cell line	Survival days	Tumor formation*	Ascites†	Disseminated metastasis				Lymph node	Liver	Pancreas‡	Kidney‡
				Omentum	Mesenterium	Peritoneum	Diaphragm				
44As3	35 ± 15 (22-65)	15/15 (100%)	14/15 (93%)	15/15	15/15	15/15	9/15	15/15	10/15	6/15	1/15
HSC-44PE	135 ± 48 (90-200)	10/15 (67%)	0/10 (0%)	5/10	3/10	3/10	0/10	5/10	0/10	0/10	0/10

*Mice were sacrificed 200 days after the orthotopic implantation. Data are the number of mice bearing metastases at the site/total number of mice bearing tumor.
†Ascites formation: >0.5 mL of ascitic fluid.
‡Micrometastases.

Table 2. Detection of metastasis and peritoneal dissemination after the orthotopic implantation of 44As3 cells

Days	Stomach	Ascites*	Disseminated metastasis				Lymph node	Liver	Pancreas†	Kidney†
			Omentum	Mesenterium	Peritoneum	Diaphragm				
7	5/5	0/5	0/5	0/5	0/5	0/5	0/5	0/5	0/5	0/5
14	5/5	0/5	3/5	0/5	0/5	0/5	1/5†	0/5	1/5	0/5
21	5/5	1/5	5/5	3/5	3/5	0/5	2/5	1/5	1/5	0/5
28	5/5	3/5	5/5	5/5	5/5	2/5	5/5	1/5	2/5	0/5
35	5/5	5/5	5/5	5/5	5/5	3/5	5/5	2/5	2/5	1/5

*Ascites formation: >0.5 mL of ascitic fluid.
†Micrometastases.

sacrificed and subjected to postmortem examination for macroscopic, histopathologic, and ultrastructural analyses (Table 2; Fig. 2). The metastatic cells (44As3) proliferated actively in the submucous tissue of the stomach (Fig. 2*A*) and began to infiltrate in the lymphatics on the 7th day. During the 2nd week following transplantation, the tumor grew more rapidly within the gastric wall, with invasion of the muscularis propria and the subserosal tissue (Fig. 2*B*). In some mice showing rapid growth of the tumor, the cancer cells broke through the serosa to become exfoliated and freed (Fig. 2*C*). These exfoliated and freed cancer cells could be visualized under the scanning electron microscope (Fig. 2*D* and *E*). Peritoneal dissemination began to be noted in the 2nd week, with cells on the greater omentum (Table 2). Micrometastases to the lymph nodes and pancreas were also noted, although not frequently. By the 3rd week, the foci of metastasis were noted in the greater omentum, mesenterium, and peritoneum. Scanning electron microscopy revealed the proliferation of the cancer cells (e.g., those colonizing the mesenterium) with the formation of larger cell clusters (data not shown). In the peritoneum, colonization of the freed cancer cells and their interaction with

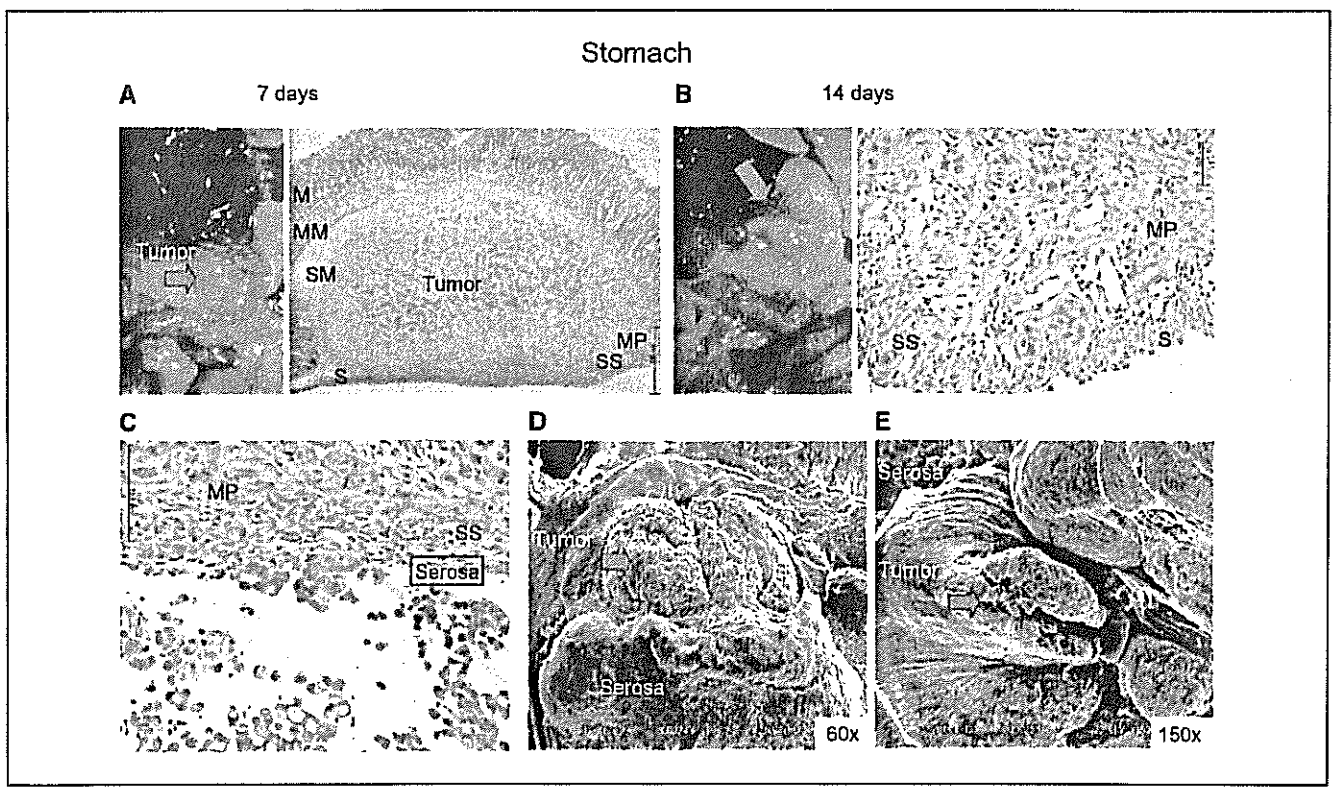

Figure 2. Macroscopic and microscopic appearance of the tumor growth of stomach of nude mice after orthotopic implantation of 44As3 cells. *A, green arrow,* orthotopic implantation of 44As3 cells in the stomach of nude mice was followed by tumor formation 7 days later. Actively proliferating 44As3 cells in the gastric submucosa (H&E). *M,* mucosa; *MM,* muscularis mucosae; *SM,* submucosa; *MP,* muscularis propria; *SS,* subserosa; *S,* serosa. *B,* tumor invasion of the muscularis propria and subserosal tissue (H&E). *C,* note 44As3 cells breaking through the serosa and becoming exfoliated and free (H&E). *D* and *E,* visualization of cancer cells breaking through the serosa and becoming exfoliated and free. Mice were sacrificed, and the tissues were examined for metastasis in various organs and processed for histologic examination as described (47, 48). Scanning electron microscopic examination was done according to standard procedures (49).

mesothelial cells were visualized (data not shown). By the 4th week, metastases to the greater omentum, mesenterium, peritoneum, and lymph nodes were noted and some animals also showed additional metastasis to the diaphragm (Table 2). Metastasis to the liver was occasionally seen. In some mice, in which the tumors grew rapidly, formation of ascites began to be noted ~21 days after the orthotopic implantation. Some of these animals became moribund on the 28th day (Tables 1 and 2). By the 35th day, all the animals showed metastasis, with dissemination to the greater omentum, mesenterium, and peritoneum accompanied by the formation of bloody ascites as well as lymph node metastasis (Table 2). Metastasis to the diaphragm was also seen frequently. Micrometastasis to the kidneys was noted in a few animals.

Analysis of the progression of dissemination using luciferase gene–tranfected cells. The analytic method described above allows detailed evaluation even of micrometastases. However, it has limitations from the viewpoint of quantitative and objective analysis. To resolve these problems, we introduced the luciferase gene into the metastatic 44As3 cell line and its parent cell line HSC-44PE by means of liposome transfer; this yielded cells with high luciferase activity, 44As3Luc and HSC44Luc, respectively. When the 44As3Luc cells (1×10^6/100 μL) were implanted s.c. into nude mice, a significant correlation was observed between tumor growth (volume) and the luciferase emission level (photon number; Fig. 3). Both cell lines were therefore used for the subsequent experiments.

The metastatic 44As3Luc or its parent cell line HSC44Luc cells were implanted orthotopically into nude mice. With the light emission noted at the site of implantation, photon counting analysis was thereafter carried out at intervals of 3 or 4 days. Figure 4*A* (*top*) presents a typical example. Chronological observation of the same animals, which were kept alive, was possible by this method. The 44As3Luc cells proliferated actively in the stomach. By the 15th day after implantation, tumor invasion of the peritoneal cavity and gradual progression of dissemination and increases in the sizes of the cell clusters were observed. Around the 25th day after implantation, a marked increase in the volume of the ascitic pool was noted by macroscopic observation, and some moribund mice were observed after the 29th day. When the moribund animals were sacrificed for autopsy, dissemination to the mesenterium and parietal peritoneum was often observed, frequently accompanied by metastasis to the lymph nodes. It was confirmed anatomically and histopathologically that the light-emitting sites corresponded to the tumor-affected sites (Fig. 4*B*). On the other hand, in the animals transplanted with the HSC44Luc, the tumor growth tended to be confined to the region of the stomach where the cells had been implanted (Fig. 4*B*), with slower tumor cell proliferation. As shown in Fig. 4*A* (*bottom*), luminescence was sometimes noted in the lymph nodes around the stomach and so on, but all of these foci of metastasis had regressed by ~60 days after implantation. Moribund animals began to be observed by the 85th day, although no ascites formation was noted in any of the animals.

By plotting the number of photons against time, a tumor growth curve reflecting the progression of peritoneal dissemination was obtained. When the relative number of photons from the highly metastatic cell line 44As3Luc and its parent cell line HSC44Luc (relative to the number of photons immediately after transplantation = 100) was plotted against time, quantitative comparison of the extents of proliferation of the two cell lines with different metastasizing potentials was possible (Fig. 4*C*).

Evaluation of the possibility of quantitative and objective screening of the effectiveness of anticancer agents. In a previous study, tumor growth was found to be suppressed in animals given i.v. injections of CPT-11, resulting in a significant prolongation

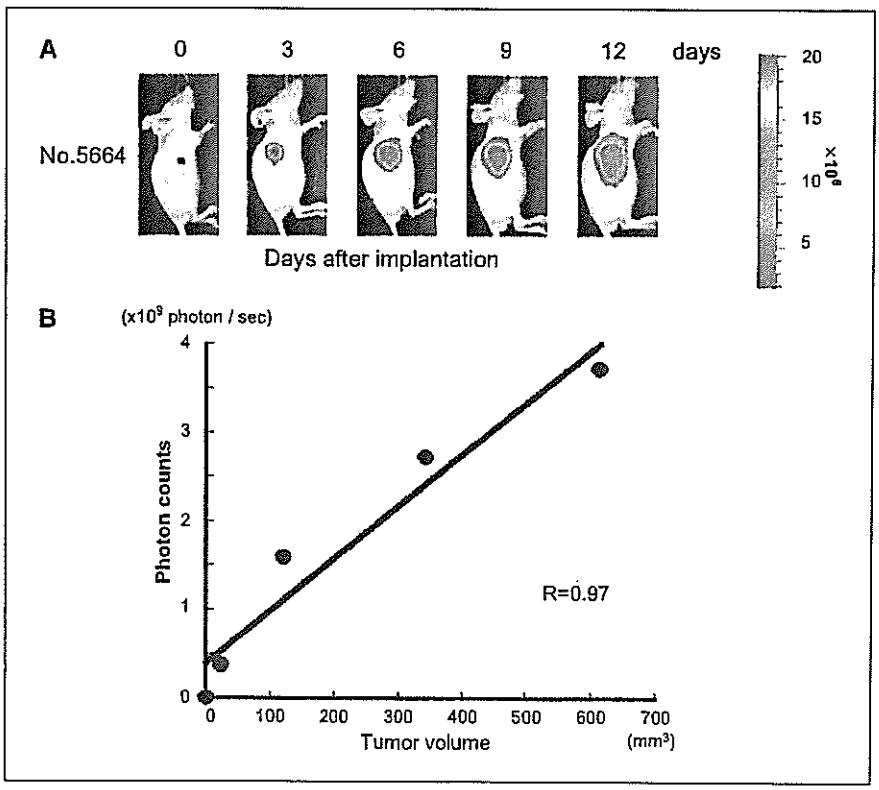

Figure 3. Correlation between the photon counts and tumor volume. *A*, nude mice bearing 44As3Luc tumors in the s.c. were visualized in anesthetized animals after i.p. inoculation of luciferin. *B*, correlation plot; strong correlation ($R = 0.97$) was observed between the conventional methods and our photon counting analysis method for monitoring the growth of a s.c. 44As3Luc tumor ($n = 5$). The tumor mass was measured at predetermined time intervals in two dimensions with calipers, and the tumor volume was calculated according to the equation $(l \times w^2) / 2$, where l is the length and w is the width (16).